

# ENGINEERING OF BIOMATERIALS

INŻYNIERIA BIOMATERIAŁÓW

JOURNAL OF POLISH SOCIETY FOR BIOMATERIALS AND FACULTY OF MATERIALS SCIENCE AND CERAMICS AGH-UST

CZASOPISMO POLSKIEGO STOWARZYSZENIA BIOMATERIAŁÓW I WYDZIAŁU INŻYNIERII MATERIAŁOWEJ I CERAMIKI AGH

**Number 151**

Numer 151

**Volume XXII**

Rok XXII

**JULY 2019**

LIPIEC 2019

**ISSN 1429-7248**

**PUBLISHER:**

WYDAWCA:

**Polish Society  
for Biomaterials  
in Krakow**

Polskie  
Stowarzyszenie  
Biomateriałów  
w Krakowie

**EDITORIAL  
COMMITTEE:**

KOMITET

REDAKCYJNY:

**Editor-in-Chief**

Redaktor naczelny

**Jan Chłopek**

**Editor**

Redaktor

**Elżbieta Pamuła**

**Secretary of editorial**

Sekretarz redakcji

**Design**

Projekt

**Katarzyna Trała**

**ADDRESS OF  
EDITORIAL OFFICE:**

ADRES REDAKCJI:

**AGH-UST**

30/A3, Mickiewicz Av.

30-059 Krakow, Poland

Akademia

Górnictwo-Hutnicza

al. Mickiewicza 30/A-3

30-059 Kraków

**Issue: 250 copies**

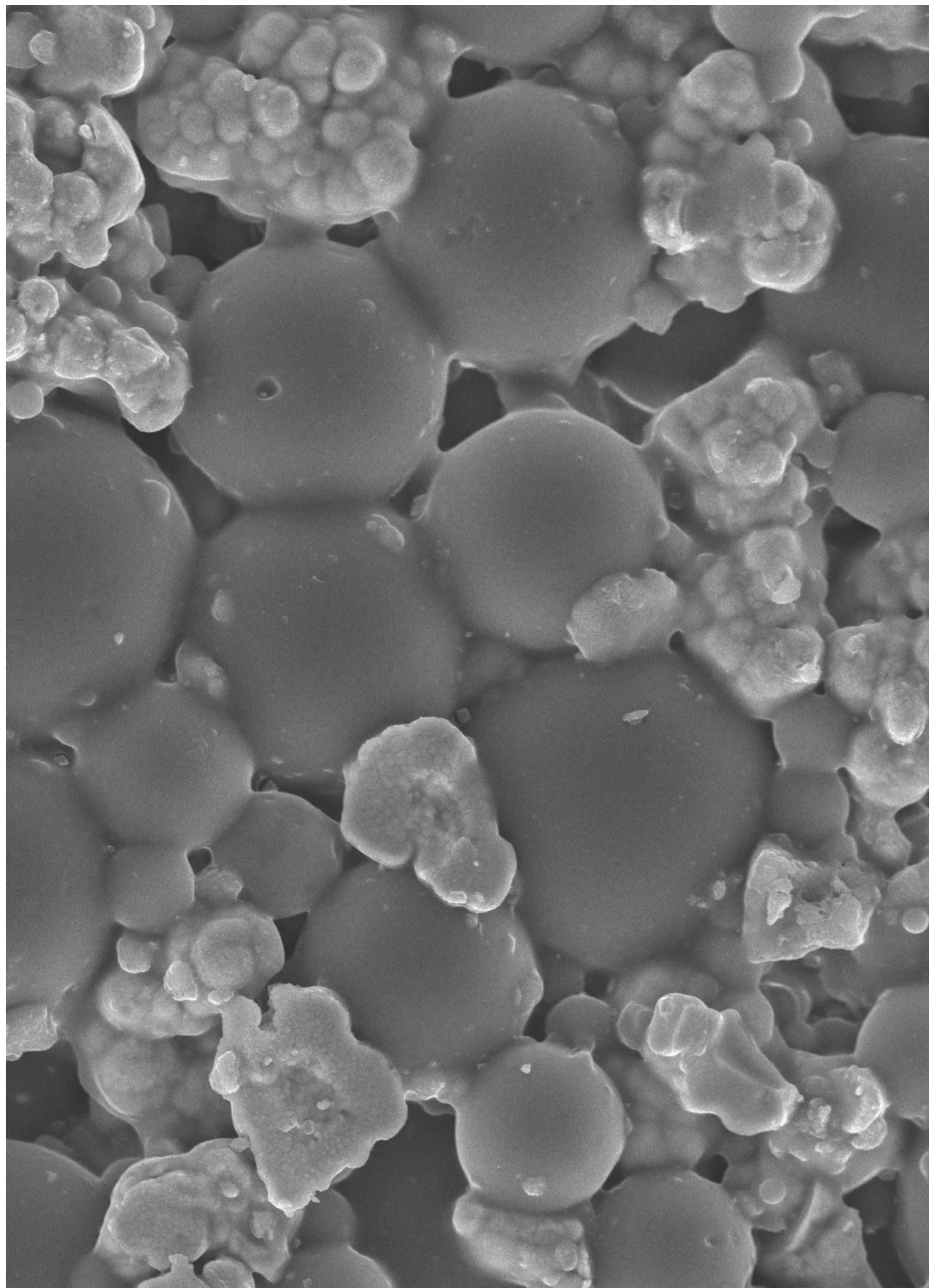
Nakład: 250 egz.

**Scientific Publishing  
House AKAPIT**

Wydawnictwo Naukowe

AKAPIT

e-mail: wn@akapit.krakow.pl



**EDITORIAL BOARD  
KOMITET REDAKCYJNY**

**EDITOR-IN-CHIEF**

Jan Chłopek - AGH UNIVERSITY OF SCIENCE AND TECHNOLOGY, KRAKOW, POLAND

**EDITOR**

Elżbieta Pamuła - AGH UNIVERSITY OF SCIENCE AND TECHNOLOGY, KRAKOW, POLAND

**INTERNATIONAL EDITORIAL BOARD  
MIĘDZYNARODOWY KOMITET REDAKCYJNY**

Iulian Antoniac - UNIVERSITY POLITEHNICA OF BUCHAREST, ROMANIA

Lucie Bacakova - ACADEMY OF SCIENCE OF THE CZECH REPUBLIC, PRAGUE, CZECH REPUBLIC

Romuald Będziński - UNIVERSITY OF ZIELONA GÓRA, POLAND

Marta Błażewicz - AGH UNIVERSITY OF SCIENCE AND TECHNOLOGY, KRAKOW, POLAND

Stanisław Błażewicz - AGH UNIVERSITY OF SCIENCE AND TECHNOLOGY, KRAKOW, POLAND

Maria Borczuch-Łączka - AGH UNIVERSITY OF SCIENCE AND TECHNOLOGY, KRAKOW, POLAND

Wojciech Chrzanowski - UNIVERSITY OF SYDNEY, AUSTRALIA

Jan Ryszard Dąbrowski - BIAŁYSTOK TECHNICAL UNIVERSITY, POLAND

Timothy Douglas - LANCASTER UNIVERSITY, UNITED KINGDOM

Christine Dupont-Gillain - UNIVERSITÉ CATHOLIQUE DE LOUVAIN, BELGIUM

Matthias Epple - UNIVERSITY OF DUISBURG-ESSEN, GERMANY

Robert Hurt - BROWN UNIVERSITY, PROVIDENCE, USA

James Kirkpatrick - JOHANNES GUTENBERG UNIVERSITY, MAINZ, GERMANY

Ireneusz Kotela - CENTRAL CLINICAL HOSPITAL OF THE MINISTRY OF THE INTERIOR AND ADMINISTR. IN WARSAW, POLAND

Małgorzata Lewandowska-Szumieł - MEDICAL UNIVERSITY OF WARSAW, POLAND

Jan Marciniak - SILESIA UNIVERSITY OF TECHNOLOGY, ZABRZE, POLAND

Ion N. Mihailescu - NATIONAL INSTITUTE FOR LASER, PLASMA AND RADIATION PHYSICS, BUCHAREST, ROMANIA

Sergey Mikhalovsky - UNIVERSITY OF BRIGHTON, UNITED KINGDOM

Stanisław Mitura - TECHNICAL UNIVERSITY OF LIBEREC, CZECH REPUBLIC

Piotr Niedzielski - TECHNICAL UNIVERSITY OF LODZ, POLAND

Abhay Pandit - NATIONAL UNIVERSITY OF IRELAND, GALWAY, IRELAND

Stanisław Pielka - WROCLAW MEDICAL UNIVERSITY, POLAND

Vehid Salih - UCL EASTMAN DENTAL INSTITUTE, LONDON, UNITED KINGDOM

Jacek Składzień - JAGIELLONIAN UNIVERSITY, COLLEGIUM MEDICUM, KRAKOW, POLAND

Andrei V. Stanishevsky - UNIVERSITY OF ALABAMA AT BIRMINGHAM, USA

Anna Ślósarczyk - AGH UNIVERSITY OF SCIENCE AND TECHNOLOGY, KRAKOW, POLAND

Tadeusz Trzaska - UNIVERSITY SCHOOL OF PHYSICAL EDUCATION, POZNAŃ, POLAND

Dimitris Tsipas - ARISTOTLE UNIVERSITY OF THESSALONIKI, GREECE

## Wskazówki dla autorów

1. Prace do opublikowania w kwartalniku „Engineering of Biomaterials / Inżynieria Biomateriałów” przyjmowane będą wyłącznie w języku angielskim. Możliwe jest również dołączenie dodatkowo polskiej wersji językowej.

2. Wszystkie nadsyłane artykuły są recenzowane.

3. Materiały do druku prosimy przysyłać na adres e-mail: kabe@agh.edu.pl.

4. Struktura artykułu:

• TYTUŁ • Autorzy i instytucje • Streszczenie (200-250 słów) • Słowa kluczowe (4-6) • Wprowadzenie • Materiały i metody • Wyniki i dyskusja • Wnioski • Podziękowania • Piśmiennictwo

5. Autorzy przesyłają pełną wersję artykułu, łącznie z ilustracjami, tabelami, podpisami i literaturą w jednym pliku. Artykuł w tej formie przesyłany jest do recenzentów. Dodatkowo autorzy proszeni są o przesłanie materiałów ilustracyjnych (rysunki, schematy, fotografie, wykresy) w oddzielnych plikach (format np. .jpg, .gif, .tiff, .bmp). Rozdzielczość rysunków min. 300 dpi. Wszystkie rysunki i wykresy powinny być czarno-białe lub w odcieniach szarości i ponumerowane cyframi arabskimi. W tekście należy umieścić odnośniki do rysunków i tabel. W przypadku artykułów dwujęzycznych w tabelach i na wykresach należy umieścić opisy polskie i angielskie.

6. Na końcu artykułu należy podać wykaz piśmiennictwa w kolejności cytowania w tekście i kolejno ponumerowany.

7. Redakcja zastrzega sobie prawo wprowadzenia do opracowań autorskich zmian terminologicznych, poprawek redakcyjnych, stylistycznych, w celu dostosowania artykułu do norm przyjętych w naszym czasopiśmie. Zmiany i uzupełnienia merytoryczne będą dokonywane w uzgodnieniu z autorem.

8. Opinia lub uwagi recenzentów będą przekazywane Autorowi do ustosunkowania się. Nie dostarczenie poprawionego artykułu w terminie oznacza rezygnację Autora z publikacji pracy w naszym czasopiśmie.

9. Za publikację artykułów redakcja nie płaci honorarium autorskiego.

10. Adres redakcji:

Czasopismo

„Engineering of Biomaterials / Inżynieria Biomateriałów”

Akademia Górniczo-Hutnicza im. St. Staszica

Wydział Inżynierii Materiałowej i Ceramiki

al. Mickiewicza 30/A-3, 30-059 Kraków

tel. (48) 12 617 25 03, 12 617 25 61

tel./fax: (48) 12 617 45 41

e-mail: chlopek@agh.edu.pl, kabe@agh.edu.pl

Szczegółowe informacje dotyczące przygotowania manuskryptu oraz procedury recenzowania dostępne są na stronie internetowej czasopisma:

**www.biomat.krakow.pl**

## Warunki prenumeraty

Zamówienie na prenumeratę prosimy przysyłać na adres:

mgr inż. Augustyn Powroźnik

apowroz@agh.edu.pl, tel/fax: (48) 12 617 45 41

Cena pojedynczego numeru wynosi 20 PLN

Konto: Polskie Stowarzyszenie Biomateriałów

30-059 Kraków, al. Mickiewicza 30/A-3

ING Bank Śląski S.A. O/Kraków

nr rachunku 63 1050 1445 1000 0012 0085 6001

Prenumerata obejmuje 4 numery regularne i nie obejmuje numeru specjalnego (materiały konferencyjne).

## Instructions for authors

1. Papers for publication in quarterly journal „Engineering of Biomaterials / Inżynieria Biomateriałów” should be written in English.

2. All articles are reviewed.

3. Manuscripts should be submitted to editorial office by e-mail to kabe@agh.edu.pl.

4. A manuscript should be organized in the following order:  
• TITLE • Authors and affiliations • Abstract (200-250 words)  
• Keywords (4-6) • Introduction • Materials and Methods • Results and Discussions • Conclusions • Acknowledgements  
• References

5. All illustrations, figures, tables, graphs etc. preferably in black and white or grey scale should be additionally sent as separate electronic files (format .jpg, .gif, .tiff, .bmp). High-resolution figures are required for publication, at least 300 dpi. All figures must be numbered in the order in which they appear in the paper and captioned below. They should be referenced in the text. The captions of all figures should be submitted on a separate sheet.

6. References should be listed at the end of the article. Number the references consecutively in the order in which they are first mentioned in the text.

7. The Editors reserve the right to improve manuscripts on grammar and style and to modify the manuscripts to fit in with the style of the journal. If extensive alterations are required, the manuscript will be returned to the authors for revision.

8. Opinion or notes of reviewers will be transferred to the author. If the corrected article will not be supplied on time, it means that the author has resigned from publication of work in our journal.

9. Editorial does not pay author honorarium for publication of article.

10. Address of editorial office:

Journal

„Engineering of Biomaterials / Inżynieria Biomateriałów”

AGH University of Science and Technology

Faculty of Materials Science and Ceramics

30/A-3, Mickiewicz Av., 30-059 Krakow, Poland

tel. (48) 12) 617 25 03, 12 617 25 61

tel./fax: (48) 12 617 45 41

e-mail: chlopek@agh.edu.pl, kabe@agh.edu.pl

Detailed information concerning manuscript preparation and review process are available at the journal's website:

**www.biomat.krakow.pl**

## Subscription terms

Contact:

MSc Augustyn Powroźnik,

e-mail: apowroz@agh.edu.pl

Subscription rates:

Cost of one number: 20 PLN

Payment should be made to:

Polish Society for Biomaterials

30/A3, Mickiewicz Av.

30-059 Krakow, Poland

ING Bank Śląski S.A.

account no. 63 1050 1445 1000 0012 0085 6001

Subscription includes 4 issues and does not include special issue (conference materials).



# 28<sup>th</sup> Biomaterials in Medicine and Veterinary Medicine Annual Conference

10 – 13 October 2019 Ryty, Poland

SAVE THE DATE

10-13

OCTOBER  
2019

[www.biomat.agh.edu.pl](http://www.biomat.agh.edu.pl)



REGISTER  
AND  
SUBMIT  
AN ABSTRACT





.....

## STUDIA PODYPLOMOWE

### Biomateriały – Materiały dla Medycyny 2019/2020

<b>Organizator:</b> Akademia Górniczo-Hutnicza im. Stanisława Staszica w Krakowie Wydział Inżynierii Materiałowej i Ceramiki Katedra Biomateriałów i Kompozytów	<b>Adres:</b> 30-059 Kraków, Al. Mickiewicza 30 Pawilon A3, p. 208, 210 lub 501 tel. 12 617 44 48, 12 617 23 38, fax. 12 617 33 71 email: epamula@agh.edu.pl; krok@agh.edu.pl
<b>Kierownik:</b> prof. dr hab. inż. Elżbieta Pamuła <b>Sekretarz:</b> dr inż. Małgorzata Krok-Borkowicz	<a href="https://www.agh.edu.pl/ksztalcenie/oferta-ksztalcenia/studia-podyplomowe-kursy-dokształcające-i-szkolenia/biomateriały-materiały-dla-medycyny/">https://www.agh.edu.pl/ksztalcenie/oferta-ksztalcenia/ studia-podyplomowe-kursy-dokształcające-i-szkolenia/ biomateriały-materiały-dla-medycyny/</a>
<b>Charakterystyka:</b> Tematyka prezentowana w trakcie zajęć obejmuje przegląd wszystkich grup materiałów dla zastosowań medycznych: metalicznych, ceramicznych, polimerowych, węglowych i kompozytowych. Słuchacze zapoznają się z metodami projektowania i wytwarzania biomateriałów a następnie możliwościami analizy ich właściwości mechanicznych, właściwości fizykochemicznych (laboratoria z metod badań: elektronowa mikroskopia skaningowa, mikroskopia sił atomowych, spektroskopia w podczerwieni, badania energii powierzchniowej i zwilżalności) i właściwości biologicznych (badania: <i>in vitro</i> i <i>in vivo</i> ). Omawiane są regulacje prawne i aspekty etyczne związane z badaniami na zwierzętach i badaniami klinicznymi (norma EU ISO 10993). Słuchacze zapoznają się z najnowszymi osiągnięciami w zakresie nowoczesnych nośników leków, medycyny regeneracyjnej i inżynierii tkankowej.	
<b>Sylwetka absolwenta:</b> Studia adresowane są do absolwentów uczelni technicznych (inżynieria materiałowa, technologia chemiczna), przyrodniczych (chemia, biologia, biotechnologia) a także medycznych, stomatologicznych, farmaceutycznych i weterynaryjnych, pragnących zdobyć, poszerzyć i ugruntować wiedzę z zakresu inżynierii biomateriałów i nowoczesnych materiałów dla medycyny. Słuchacze zdobywają i/lub pogłębiają wiedzę z zakresu inżynierii biomateriałów. Po zakończeniu studiów wykazują się znajomością budowy, właściwości i sposobu otrzymywania materiałów przeznaczonych dla medycyny. Potrafią analizować wyniki badań i przekładać je na zachowanie się biomateriału w warunkach żywego organizmu. Ponadto słuchacze wprowadzani są w zagadnienia dotyczące wymagań normowych, etycznych i prawnych niezbędnych do wprowadzenia nowego materiału na rynek. Ukończenie studiów pozwala na nabycie umiejętności przygotowywania wniosków do Komisji Etycznych i doboru metod badawczych w zakresie analizy biogodności materiałów.	
<b>Zasady naboru:</b> Termin zgłoszeń: od 20.09.2019 do 20.10.2019 (liczba miejsc ograniczona - decyduje kolejność zgłoszeń) Wymagane dokumenty: dyplom ukończenia szkoły wyższej Osoby przyjmujące zgłoszenia: prof. dr hab. inż. Elżbieta Pamuła (pawilon A3, p. 208, tel. 12 617 44 48, e-mail: epamula@agh.edu.pl) dr inż. Małgorzata Krok-Borkowicz (pawilon A3, p. 210, tel. 12 617 23 38, e-mail: krok@agh.edu.pl)	
<b>Czas trwania:</b> 2 semestry (od XI 2019 r. do VI 2020 r.) 8 zjazdów (soboty-niedziele) 1 raz w miesiącu	<b>Opłaty:</b> 2 600 zł (za dwa semestry)

.....

## SPIS TREŚCI CONTENTS

<b>MECHANICAL AND BIOLOGICAL          PROPERTIES OF CARBON FIBER-          REINFORCED PEEK COMPOSITE          MATERIALS INTENDED FOR          LARYNGEAL PROSTHESES</b> WOJCIECH SMÓŁKA, MICHAŁ DWORAK, BARTŁOMIEJ NOWORYTA, MACIEJ GUBERNAT, JAROSŁAW MARKOWSKI, MARTA BŁAŻEWICZ	<b>2</b>
<b>CHANGES OF STRUCTURE AND          PROPERTIES OF PMMA-BASED BONE          CEMENTS WITH HYDROXYAPATITE          AFTER DEGRADATION PROCESS</b> ANNA LASKA-LEŚNIEWICZ, MAŁGORZATA RACZYŃSKA, MACIEJ WROTNIK, ANNA SOBCZYK-GUZENDA	<b>9</b>
<b>SURFACE MODIFICATIONS FOR INFLOW          CANNULAS OF VENTRICULAR ASSIST          DEVICES – COMPARISON          OF LATEST SOLUTIONS</b> PRZEMYSŁAW KURTYKA, ROMAN KUSTOSZ, MARCIN KACZMAREK, MAŁGORZATA GONSIOR, KLAUDIA TOKARSKA	<b>17</b>
<b>OSTEOBLASTS RESPONSE TO NOVEL          CHITOSAN/AGAROSE/HYDROXYAPATITE          BONE SCAFFOLD – STUDIES ON          MC3T3-E1 AND HFOB 1.19          CELLULAR MODELS</b> PAULINA KAZIMIERCZAK, VLADYSLAV VIVCHARENKO, WIESŁAW TRUSZKIEWICZ, MICHAŁ WÓJCIK, AGATA PRZEKORA	<b>24</b>

# MECHANICAL AND BIOLOGICAL PROPERTIES OF CARBON FIBER-REINFORCED PEEK COMPOSITE MATERIALS INTENDED FOR LARYNGEAL PROSTHESES

WOJCIECH SMÓŁKA<sup>1</sup> , MICHAŁ DWORAK<sup>2</sup> ,  
BARTŁOMIEJ NOWORYTA<sup>3</sup>, MACIEJ GUBERNAT<sup>3</sup> ,  
JAROSŁAW MARKOWSKI<sup>1</sup> , MARTA BŁĄŻEWICZ<sup>3\*</sup> 

<sup>1</sup> MEDICAL UNIVERSITY OF SILESIA IN KATOWICE,  
SCHOOL OF MEDICINE IN KATOWICE,  
LARYNGOLOGY DEPARTMENT,  
UL. MEDYKÓW 18, 40-752 KATOWICE, POLAND

<sup>2</sup> UNIVERSITY OF SILESIA, FACULTY OF COMPUTER SCIENCE  
AND MATERIALS SCIENCE, INSTITUTE OF MATERIALS SCIENCE,  
UL. 75 PUŁKU PIECHOTY 1A, 41-500 CHORZÓW, POLAND

<sup>3</sup> AGH UNIVERSITY OF SCIENCE AND TECHNOLOGY,  
FACULTY OF MATERIALS SCIENCE AND CERAMICS,  
AL. MICKIEWICZA 30, 30-059 KRAKOW, POLAND

\*E-MAIL: MBLAZEW@AGH.EDU.PL

## Abstract

*The work deals with the mechanical properties and biological behaviour of composite materials made of polyether ether ketone (PEEK) polymer and carbon fibers (CF) designed for laryngeal biomaterials. Two types of PEEK-based matrix composites containing carbon fibers in the form of cloth (2D) and short fibers (MD) were made. The composite samples were obtained via hot molding of PEEK/CF prepregs. Mechanical durability of the composite samples aging in Ringer's solution at 37°C was analyzed. The samples were dynamically loaded under bending force up to 10<sup>6</sup> cycles. The ultrasonic wave propagation method was applied to study changes in the composites. The mechanical changes were analyzed, taking into consideration the anisotropic structure of the composite samples. The layered composite samples were modified with multiwalled carbon nanotubes (CNTs). The changes in mechanical stability of the composite samples were not significant after fatigue testing up to 1 · 10<sup>6</sup> cycles. The biological tests were carried out in the presence of hFOB-1.19-line human osteoblasts and HS-5-line human fibroblasts. The level of type I collagen produced from both types of cells was determined by ELISA test. The tests showed differences between the samples with regard to the viability of the cells.*

**Keywords:** composite materials; PEEK, mechanical properties, cells viability

[*Engineering of Biomaterials* 151 (2019) 2-8]

## Introduction

Larynx is a key element of the upper respiratory tract that ensures free airflow towards the trachea and bronchi. It also plays an important role in creating voice and speech. Larynx cancer is the most common squamous cell carcinoma in the head and neck area (Head and Neck Squamous Cell Carcinoma - HNSCC). It is the seventh most frequently occurring malignant tumor in the male population in Poland, and according to the National Cancer Registry data in 2010, 2,200 new cases of this cancer were found, and more than 1,500 people died [1].

In the case of patients with high clinical advancement of larynx cancer, the most common treatment is total laryngectomy, i.e. removal of the larynx. After the surgery, the respiratory tract is changed. The airflow begins at the trachea level, and the inhaled air is not cleaned, as it is during its natural flow through the nose and throat. In addition, without larynx, a patient is deprived of the basic organ to create the voice.

For many years, voice prostheses have been used to rehabilitate the speech of laryngectomized patients. The prosthesis implantation involves creating a fistula communicating the trachea with the esophagus, which enables the development of tracheoesophageal speech. Within the obtained fistula a voice prosthesis is placed which functions as a unilateral valve system. The esophagus oscillations caused by the airflow are then transmitted to the throat and mouth where they are transformed into intelligible speech [2-4]. In Poland, the most commonly used silicone prostheses are Provox (Atos Medical AB, Hörby, Sweden) and Blom-Singer (InHealth Technologies, Carpinteria, CA, USA). The voice prosthesis functionality in the specific environment of tracheal mucosa and esophagus is characterized by limited "vitality". Implanted prostheses require periodic replacement due to their deteriorated quality and reduced functioning. The prosthesis lifetime, voice quality and ease of voicing are important factors when choosing the voice prosthesis. According to literature data, the average lifetime of an implanted prosthesis is 3-6 months [2,4,5]. After this time, the prosthesis needs to be replaced. The limitation in the functioning of the prosthesis is caused by the following factors: the properties of the prosthesis itself, i.e., mechanical dysfunction of the valve system resulting from the biofilm formation, and the properties of tissues surrounding the fistula, such as superinfection of the implantation site, formation of granulation tissue around the prosthesis or the fistula enlargement leading to its expulsion to the esophagus or trachea, which involves the risk of bronchial aspiration and life-threatening complications [2,6,7].

The basic features that determine the prosthesis viability include the quality of the material (usually silicone) and the efficiency and strength of the valve system. The most disadvantageous phenomenon impairing the voice prosthesis functionality is the biofilm formed on the silicon surface of the prosthetic valve which changes its kinetic properties. The biofilm is a specialized colony of bacteria and/or fungi that produce an extracellular matrix.

Therefore, the inhibition of biofilm formation is researched to improve the durability of voice prostheses. One of the considered solutions is using silicone enriched with a 7% addition of silver oxide which is known for its bactericidal properties. An example of the prosthesis endowed with bacteriostatic properties of silver oxide is Blom-Singer® Dual Valve™ [8]. The tracheal mucosal damage can lead to granulation around the tracheo-esophageal fistula. Therefore, the appropriate design of the prosthesis that minimizes the risk of mucosal damage may extend its lifetime. Such a modification is used in Provox® Vega™ prostheses which are made of PTFE polymers [9].

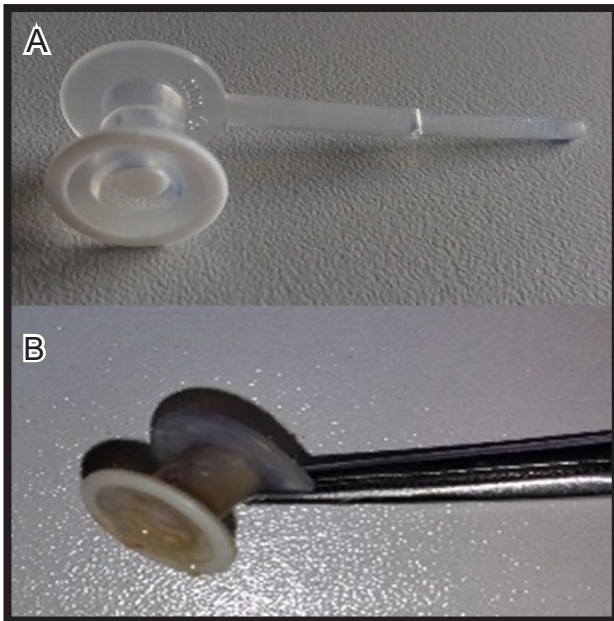


**FIG. 1. Voice prostheses used in laryngology: A - Blom-Singer voice prosthesis before surgery; American company INHEALTH®I, B - Worn off Blom-Singer voice prosthesis after removal from tracheoesophageal fistula.**

FIG. 1 shows the voice prosthesis before surgery (A) and after removal from the larynx (B).

The prosthesis dysfunction caused by losing the proper airflow pressure in the valve system impairs the effective formation of the tracheo-thoracic speech. The Provox® ActiValve™ prosthesis, which uses a magnet-enhanced valve mechanism, is designed to counteract the persistent early loss of such optimal kinetic values [8].

One of the possible developments of the voice prosthesis may be fibrous composite materials with appropriate fibers added to the polymer matrix. Proper manufacturing methods may also ensure the desired mechanical and biological properties. Polymer composites are compatible with modern diagnostic techniques (CT, NMR). Non-metallic composite materials seem to be a particularly good candidate to replace both pure polymer-based implants and the metallic ones used in various medical areas [10-13]. Studies have shown that the PEEK polymer matrix is endowed with properties inhibiting the biofilm formation at the implantation site [14,15]. The composites manufactured from various types of carbon fibers and PEEK matrix offer several opportunities to design and develop implants better suited for the specific treatment. As light materials, the composites can provide a high degree of anisotropy, due to physical properties similar to the replaced tissue. Optimal physical and mechanical properties of the composite which replaces the tissue or enhances the impaired organ functionality can be significantly improved by using fibrous reinforcement of roving or woven fabrics, braided fibers, fibrous sleeves, as well as chopped fibers. All those forms of the carbon fiber reinforcements appear to be beneficial for various structural applications, such as tubular implants, components of total hip prostheses, laryngeal implants and for fracture fixation joints [16-19].

However, there have not been enough experimental studies on the mechanical durability of PEEK/CF-based composites in the biological environment. In particular, the durability of such composites under dynamic loads in biological environment is a challenge that should be assessed to recognize their potential as structural implants.

The aim of the study was to manufacture composites of PEEK and carbon fiber reinforcements and to assess their mechanical strength under dynamic loading conditions and biological behavior *in vitro*. Cloths made of commercially available carbon fibers and mats of laboratory prepared PAN-based carbon fibers - were used as reinforcements. The target shapes of the composite samples were plates for laryngology. The study continues the hitherto research on the PEEK-reinforced carbon fibers composites as structural composite materials for general surgery and orthopaedics [19,20].

## Materials and Methods

### Manufacture of composite samples

The following material components were used to manufacture the composite samples:

- powder of polyether ether ketone (PEEK 150PF) delivered by Victrex was used as the matrix (TABLE 1). The Victrex polyether ether ketone for medical applications is available on the market under the separate InviBio brand as the PEEK Optima product line. The polymer is characterized by a high chemical purity and is certified by the FDA (Food and Drug Administration), and CE (a sign of compliance with the European Union New Approach Directives in the field of Active Medical Implants) to be used in implantable medicine. The polymer used in our study, under the trade name Victrex PEEK 150 PF, has identical mechanical properties and purity as the polymer for medical applications.
- (2D) carbon fiber cloths delivered from Porcher Industries Composites, code-named Pi preg® 3106-P17. The cloths in the form of prepregs were made from (2D) 3K,5H- Satin (3000 elemental fibers in roving) (TABLE 2).
- mats of laboratory manufactured PAN-based chopped carbon fibers; the thickness of the mat was 3 mm, the average fiber length in the mat was 9 mm and the tensile strength of single fiber was 0.3 GPa.
- multiwalled carbon nanotubes (CNT) provided by NanoAmor, USA. The nanotubes had diameters in the range of 10-30 nm and were 1-2  $\mu\text{m}$  long.

**TABLE 1. Victrex PEEK 150PF Product characteristics.**

Tensile Strength	100 MPa
Tensile Elongation	15%
Melting Point	343°C
Glass Transition ( $T_g$ )	143°C
Melt Viscosity (400°C)	130 Pa·s
Density	1.3 g/cm <sup>3</sup>
Bulk Density	0.3 g/cm <sup>3</sup>
Processing Temperature	380-400°C

**TABLE 2. Prepreg PEEK/2D/CF carbon cloth characteristics.**

Prepreg thickness	0.6 mm
Mass per square meter	490 g/m <sup>2</sup>
Polymer fraction in prepreg	50vo%
Polymer fraction in prepreg	43wt%
Melting Point	343°C
Glass Transition ( $T_g$ )	143°C
Processing Temperature	380-400°C



The PEEK/CF composite was processed via hot compression molding, by stacking carbon cloths. The compression molding was performed using a hydraulic press and a heated mold. 10 layers cut from the prepreg PEEK/2D cloth (0/90°) were placed in a performing mold to make the composite samples of 3.5 mm in thickness. The compression molding was carried out under the following conditions: temperature 400°C, pressure 1.5 MPa, compression time about 3 min and free cooling in the air (about 3°C/min). The optimum molding conditions were established in earlier experiments [19-21].

A part of the composite samples was additionally modified by covering the prepregs' surface with CNTs. These composite samples were manufactured, as follows: the CNTs were introduced into dimethylformaldehyde (DMF) to prepare a suspension. The suspension was homogenized with ultrasound and CNTs were spread on the carbon fiber cloths by spraying and evaporating the solvent in a laboratory dryer. The CNTs weight fraction was determined basing on the weight difference of the composite samples and the CNT amount used to produce the composite samples. Samples with the following CNT weight fraction in the composite were obtained: 0.2wt%, 0.75wt% and 1.2wt%. The composites with chopped carbon fibers were obtained by placing the reinforcement mat and spreading the predetermined amount of PEEK powdered polymer alternately. The assumed volume fraction of the matrix in the composite was about 50%. The excess of the polymer was removed from the mold during compression molding. As a result of the compression molding, the composite plates measuring 15 mm x 3 mm x 80 mm were obtained.

The following types of composite samples were manufactured:

- PEEK/2D/CF – the composite samples made of 2D carbon fiber cloths;
- PEEK/2D/CF/CNT – the composite samples made of 2D carbon fiber prepregs additionally modified with CNTs;
- PEEK/MD/CF – the composite samples made of chopped carbon fibers- reinforced PEEK.

## Methods

The mechanical properties of the composite samples were tested on a universal testing machine (Zwick 1435) controlled by TestXpert (v.8.1) software, in a bending mode. To determine the bending strength and modulus the tests were performed on the composite plates. The samples were placed on supports set 50 mm apart. The samples for bending tests measured 4 mm x 3 mm x 60 mm. The interlaminar shear strength (ILSS) of the composite samples was determined in the bending mode by short beam method with the span-to-depth ratio of 4:1. The composite plates for ILSS tests measured 3.5 mm x 3 mm x 35 mm. All the tests were conducted with a strain rate of 1 mm/min. For each type of the composite samples, 5 individual measurements were taken. The results are presented as a mean ± SD.

The fatigue properties under dynamic conditions were examined by subjecting the samples to a cyclic bending load in Ringer's solution at 37°C. The changes in the velocity of ultrasonic wave propagation in the sample were measured between consecutive cycles on the ultrasonic probe. The tests were conducted under a constant force amplitude conducted in the bending force-control mode, i.e. bending-bending mode. The level of the maximum force amplitude was established to be 50% of the strength determined in the static bending test. The samples were placed in a special reservoir containing a physiological fluid of 6.5 pH. The solution was continuously circulated by a pump system.

The samples were subjected to 10<sup>6</sup> cycles. The ultrasonic measurements were taken after each 2x10<sup>4</sup> cycles. At the beginning of the tests and between the successive stages, the wave velocity was measured. An ultrasonic tester - Ultrasonic Unipan-CT3 with heads of 1 MHz was used to measure wave propagation velocities. The mean and standard deviations of velocities were measured from 3 samples for each experimental group. For each measuring point, the velocity of the longitudinal wave propagation (CL) was determined and the value of the dynamic elastic modulus was determined from the dependence:

$$E = C_L^2 \cdot \rho \cdot K$$

where:  $C_L$  is the velocity of the longitudinal wave propagation in the sample in [m/s],  $E$  is dynamic longitudinal elasticity modulus in [GPa], and  $\rho$  is sample density, [kg/m<sup>3</sup>],  $K$  - constant, was taken to be 1. The apparent density of composite samples was determined from the weight and size measurements. The water contact angle ( $\theta$ ) of the surface samples was measured at room temperature using a DSA10, Kruss apparatus (Germany). The roughness of the surface samples was determined by the surface profilometry technique (Hommel Tester T1500). The maximum of the surface roughness height,  $R_z$  as the mean and standard deviations from 3 measurements was determined.

## Biological tests

*In vitro* experiments were carried out in the presence of hFOB-1.19-line human osteoblasts and HS-5-line human fibroblasts (ATCC, University Boulevard, Manassas, Canada). MTT tests were to determine the viability of both types of cells in the presence of the composite samples. The level of type I collagen produced from both types of cells was determined by ELISA test. The composite samples were prepared in the form of discs, 12 mm in diameter. Prior to testing, the samples were washed in 70% ethanol solution and sterilized under UV for 30 min on each side. Then, the samples were placed in the wells of the 48-well culture plates. The positive control was the polystyrene bottom of an empty culture plate well (TCPS). Cells viability was determined after a 7-day incubation, and the results were expressed as a percentage, assuming 100% of the absorbance value determined spectrometrically, at 570 nm wavelength, for the cells without the presence of the composite material.

The results were statistically analyzed using the t-test from Excel software. The p-values equal to or less than 0.05 were considered significant.

## Results and Discussion

The parameters characterizing the obtained composite samples are presented in TABLE 3.

The composite samples are characterized by similar density values and volume fractions. A slightly lower density was obtained for the composites containing short fibers. The table also presents the values of surface wettability and surface roughness of the tested materials. The surface wettability, measured as the contact angle of the samples, depends on the type of carbonaceous components and indicates that the samples with carbon fibers have higher wettability, as compared to the pure polymer. The PEEK has the  $\theta$  value characteristic for hydrophilic materials (64.4°). The composites modified with CNTs exhibit the distinctly higher values of water contact angle, i.e. 97.2-101.4°, bringing about a hydrophobic nature of the sample surface.

The mechanical properties of all types of composite samples determined in the bending test are collected in TABLE 4.

TABLE 3. Composites characteristics.

Samples	Fiber volume fraction [%]	Density [g/cm <sup>3</sup> ]	Surface roughness [ $\mu\text{m}$ ]	Water contact angle [°]
PEEK	-	1.3	8.4 $\pm$ 2.5	64.4 $\pm$ 1.3
PEEK/2D/CF	50%	1.5	46.3 $\pm$ 11.8	89.3 $\pm$ 2.3
PEEK2D/CF/CNT(0.2%)	50%	1.5	42.4 $\pm$ 8.3	97.2 $\pm$ 2.3
PEEK2D/CF/CNT(0.75%)	50%	1.5	39.4 $\pm$ 7.3	99.1 $\pm$ 3.3
PEEK2D/CF/CNT(1.2%)	50%	1.5	36.4 $\pm$ 4.3	101.4 $\pm$ 2.3
PEEK/MD/CF	45%	1.4	26.1 $\pm$ 1.2	77.3 $\pm$ 2.1

TABLE 4. Mechanical properties of PEEK- based samples.

Sample	Bending strength [MPa]	Bending modulus [GPa]	Work up to fracture [Nm]	ILSS [MPa]
PEEK	67.3 $\pm$ 5.3	2.7	-	-
PEEK/2D/CF	967.4 $\pm$ 88.7	68.6 $\pm$ 9.1	0.75 $\pm$ 0.13	57.2 $\pm$ 7.8
PEEK/2D/CF/CNT (0.2%)	887.2 $\pm$ 66.4	59.4 $\pm$ 4.8	0.82 $\pm$ 0.12	48.5 $\pm$ 3.9
PEEK/2D/CF/CNT(0.75%)	890.3 $\pm$ 26.6	65.7 $\pm$ 3.9	0.85 $\pm$ 0.06	67.3 $\pm$ 1.1
PEEK/2D/CF/CNT(1.2%)	826.6 $\pm$ 49.2	55.4 $\pm$ 4.3	0.76 $\pm$ 0.09	59.1 $\pm$ 1.1
PEEK/MD/CF	123.5 $\pm$ 17.3	5.4 $\pm$ 0.2	0.16 $\pm$ 0.1	27.8 $\pm$ 1.4

The results prove that the CNT addition causes a slight reduction in mechanical parameters, and the standard deviations of the mean values are significantly lower in the case of CNT-modified composites. It may prove a better homogeneity of these composites, especially for the samples containing 0.75% of CNTs. However, the reported content of nanotubes refers to the volume of the entire composite sample, whereas they were only deposited on the surfaces of the prepregs. For this reason, it can be assumed that nanotubes quantities at the interface boundaries between (2D) layers are higher than in the entire sample volume. The significantly lower mechanical properties were noted for the samples reinforced with short fibers. This is due to the fact that the mats of carbon fibers are characterized by low mechanical properties (tensile strength of 0.3 GPa).

For further fatigue tests, the composite samples containing 0.75wt% CNT and the unmodified composites were selected.

The manner of ultrasonic measurements of the composite plates is shown in FIG. 2. In the case of measurements along the sample (L direction), the ultrasonic heads were applied to the front surfaces of the sample. For measurements in the "a" and "b" directions, the heads were applied at three sites of the sample (FIG. 2), and the average value of 3 measurements was taken to calculate the dynamic elastic modulus.

FIG. 3 shows the changes in the dynamic elastic modulus of the CNT-modified composite plates (a) and the unmodified samples (b), respectively.

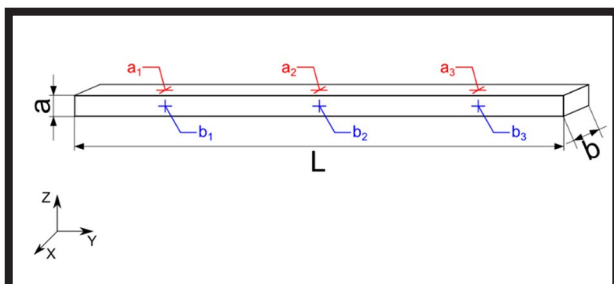


FIG. 2. Configuration of ultrasonic measurements of composite plate: L - along the length of plate, a - perpendicular to the thickness of plate, b - along the width of plate.

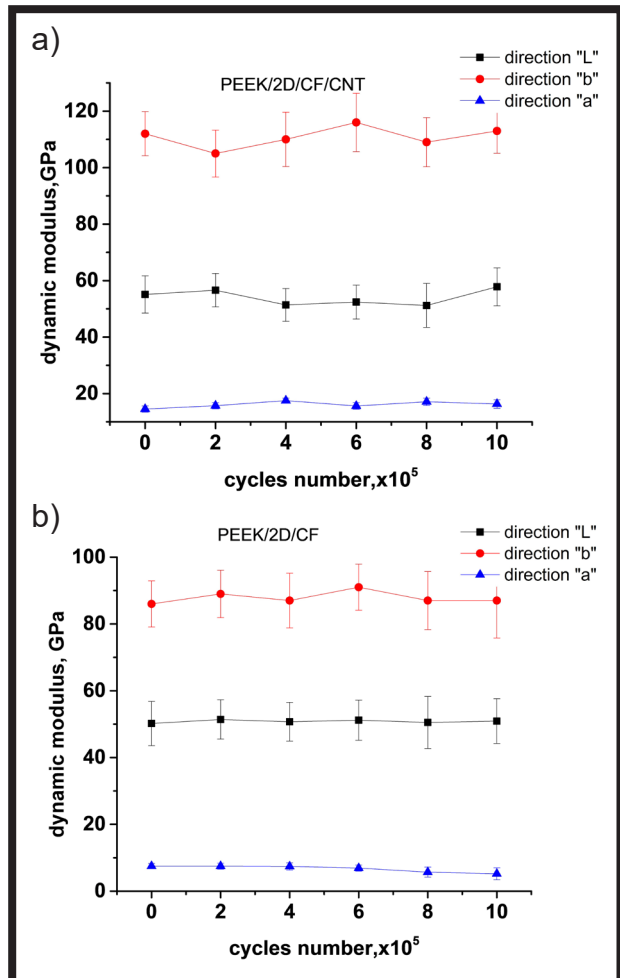


FIG. 3. Variations in dynamic elastic modulus of composite samples modified with CNT (a) and without CNT (b) as a function of cyclic load.

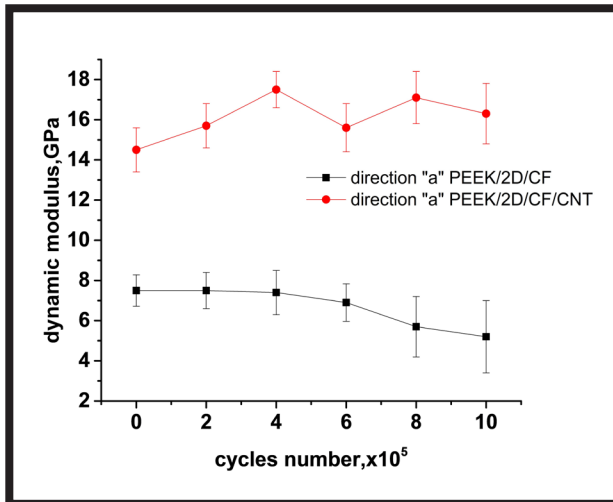


FIG. 4. Variations in dynamic elastic modulus of composite samples perpendicular to the carbon fiber layers as a function of cyclic load.

The changes in the dynamic modulus indicate that the composite samples do not degrade during dynamic loads. Due to the layered structure of the composite, it can be expected that the degradation may occur at the interlayer boundaries, which are represented by ultrasonic measurements referring to the "a" direction. The changes in the modulus in this direction do not reveal significant differences between the initial materials and after their dynamic loading to  $10^6$  cycles. However, the detailed analysis of these changes, taking into account the magnitude of the standard deviation of the ultrasonic wave propagation in the "a" direction, indicates some differences, which is shown in FIG. 4. For the composite without CNT a slight increase in SD after  $6 \times 10^5$  cycles ( $5.2 \pm 1.8$  GPa), as compared to CNT-modified composite ( $16.3 \pm 1.5$  GPa), can be observed. This may indicate the beginning of the samples' degradation. Yet, this observation requires further studies with the increased value of the load amplitude maximum.

FIGS 5-8 show the results of biological tests run on the composites with both types of carbon fibrous reinforcements and on the pure polymer samples. Cell viabilities were determined on day 7 after seeding cells on the studied materials.

*In vitro* viability tests revealed differences between the pure polymer, the composite materials, and the control. The viabilities of both types of cells were generally more favourable for the control, as compared to the pure polymer and the composite samples. Viability values for the control were taken as 100% and are not shown on the diagrams. The highest fibroblasts viability was observed on the pure polymer surface (FIG. 5), and in the case of osteoblasts the highest viability was noted for the cells cultured on the composites modified with CNT (FIG. 6). On the contrary, the lowest viability values were observed for the composites containing short carbon fibers (PEEK/MD/CF).

FIGS 7 and 8 show the level of collagen I produced by fibroblasts and osteoblasts in the presence of various composite samples.

All the PEEK-based samples were found to have a higher level of collagen I produced by osteoblasts (FIG. 8) in comparison to the control, whereas the level of collagen produced by fibroblasts was lower (FIG. 7).

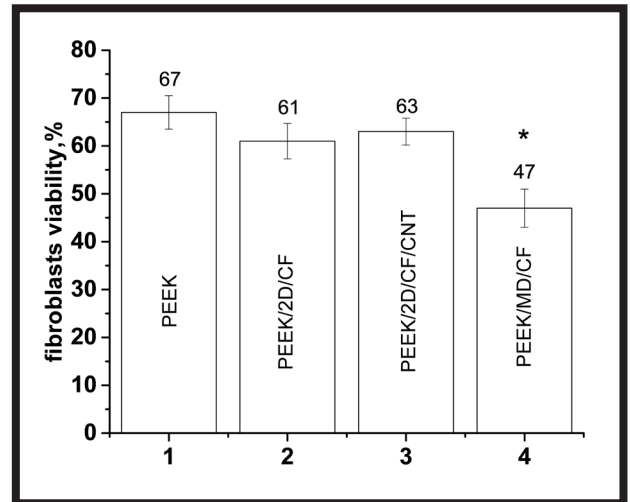


FIG. 5. Viability of HS-5-line human fibroblasts on composite surfaces on day 7 after seeding. \* statistically significant difference of PEEK-based composites on day 7 vs pure PEEK; ( $p \leq 0.05$ )

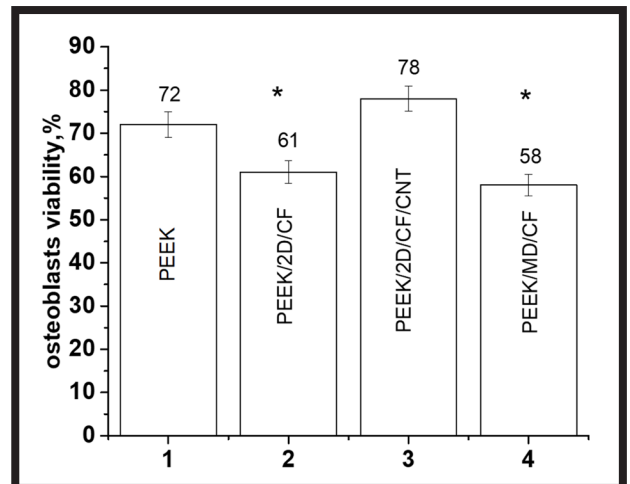
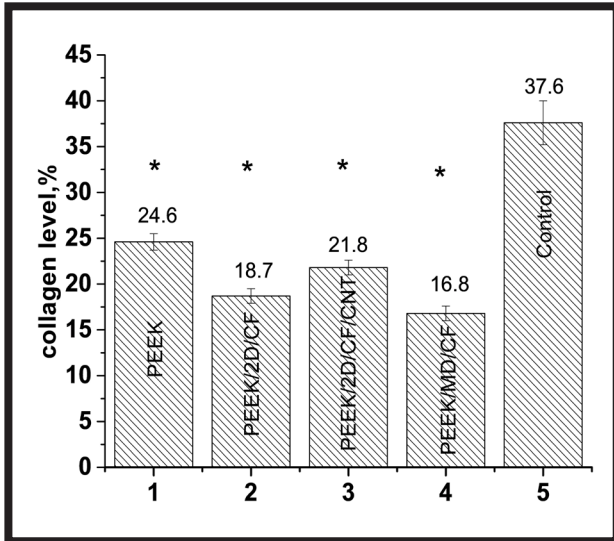


FIG. 6. Viability of hFOB-1.19-line human osteoblasts on composite surfaces on day 7 after seeding. \* statistically significant difference of PEEK-based samples on day 7 vs pure PEEK; ( $p \leq 0.05$ )

This assessment may be considered as a bioactivity test of the composite samples with respect to different cells. The results prove the influence of composite materials on osteoblasts and fibroblasts viability. The differences in viability and the level of collagen I produced by the cells may stem from the differences in the chemical and physical states of the samples' surface. The surface energy of the carbon-polymer composites is different from the pure polymers probably due to the reaction of carbon fibre surfaces with the polymer structure. The tests indicate that both types of cells are sensitive to the surface state of the composite samples.

The water contact angle measurements were performed to evaluate chemical nature of the materials surfaces. The calculated  $\theta$  values for the pure polymer material was about  $64.4^\circ$  (TABLE 3), which is characteristic for hydrophilic materials [25]. The polymer samples exhibit smaller values of the water contact angle when compared to the composite samples. The composite materials modified with CNT exhibit slightly higher values in comparison to the composites without CNT.



**FIG. 7.** Levels of collagen I produced by fibroblasts on PEEK-based sample surfaces, normalized to the level of the control.

\* statistically significant difference of PEEK-based samples on day 7 vs control; ( $p \leq 0.05$ )

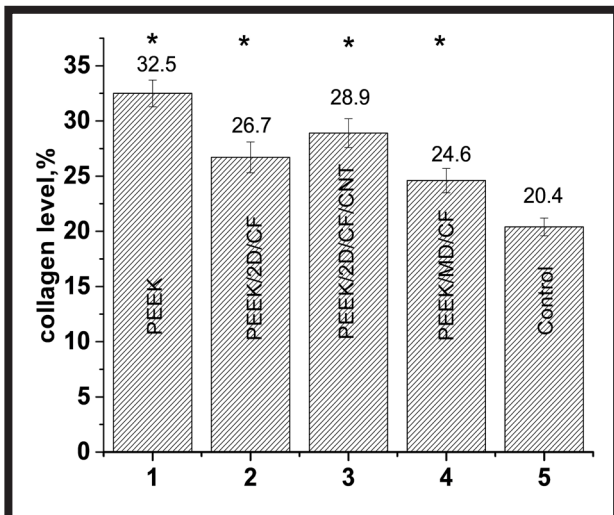


**FIG. 8.** Levels of collagen I produced by osteoblasts on PEEK-based sample surfaces normalized to the level of the control.

\* statistically significant difference of PEEK-based composites on day 7 vs control; ( $p \leq 0.05$ )

The mechanical properties of the composites differ, depending on the form of carbon fiber reinforcement. Short fibers significantly reduce the mechanical parameters of the obtained composites. Nevertheless, this type of composite can be used to manufacture composites whose layers containing chaotically arranged fibers are combined with layers containing continuous filaments. In this way, the composite structures with properties suited to a specific application can be designed. In our research, we studied two distinctly different types of composites in terms of strength properties. The use of a fibrous carbon component modifies not only the mechanical parameters of the polymer matrix, but also affects other physical and chemical properties, such as electrical properties, surface structure, and the interaction with a biological environment.

Numerous findings proved that fibrous carbon components could act as chondrogenic materials [22-24]. The carbonaceous materials, including carbon fibers and carbon nanotubes, were successfully applied in the treatment of cartilage defects. CNTs added to the polymer nanofibers improved biological and physical properties of fibrous scaffolds used for tissue engineering [25].

The study showed that the use of carbon nanotubes to modify the interface boundary between 2D layers did not enhance the mechanical properties of the composite materials. Yet, it improved the composites homogeneity, which was revealed by lowered values in the standard deviation of mechanical parameters, while the mechanical stability was maintained under dynamic loading. The fatigue bending tests at the level of variable loads (50% of maximum amplitude at which the composite fractures) indicated that such composites are durable and meet the requirements of mechanical durability for voice prostheses. Still, further tests are necessary, in particular on designing and manufacturing of the complete structure of a composite voice prosthesis.

The surface roughness, measured as the maximum of the surface roughness height, depends on the type of a carbon component and its arrangement in the polymer matrix (TABLE 3). The highest roughness was observed for the composite samples containing carbon fibrous cloths, and this parameter was significantly higher in comparison with the pure polymer.

The results of the biological tests are more complex and ambiguous. The obtained results indicate that the modification of the biocompatible polymer matrix with carbon fibers can induce significant changes in the cellular response. The research has also shown that the carbon fibers addition significantly changes the surface roughness and wettability values of the composite samples. The changes in surface properties brought about by the presence of fibers can affect the cell viability on the surface of the modified composite materials. The nanotubes introduced between the composite laminate layers increase the material hydrophobicity. Considering its prospective application for a voice prosthesis, a highly hydrophobic surface of the composite biomaterial may ensure the lack of undesirable interaction with the biological environment. Many studies on surface modification of biomaterials indicate that the use of nanometric components, e.g. various carbon nanofibers, can lead to the formation of superhydrophobic surface properties [26]. The conducted research indicated that an increase in the hydrophobicity of the composite surface may enhance the proper fixing of the biomaterial in situ. Studies have also shown that a carbon fibrous component in the polymer matrix may affect the wettability of the composite, which facilitates more efficient fitting of the composite biomaterial to the site. Another important requirement for a voice prosthesis is the ability to inhibit bacterial biofilm formation. The previous study has shown that the chemically modified PEEK surface has favorable surface properties inhibiting the development of bacterial biofilms [15].

The biological tests have shown a distinct influence of the carbon fibrous reinforcements on cells responses, and further research on the manufacturing of the composite for a voice prosthesis will be continued.

## Conclusions






The composite samples containing carbon fibers were fabricated via the compression molding method. Two combinations of carbon fiber reinforcement, i.e. carbon fiber cloth and short fibers, in the PEEK matrix were used. The composite samples were modified with CNTs. The static and fatigue properties of the composites under dynamic cyclic tests were compared for both types of materials. The samples modified with carbon nanotubes improved their homogeneity in the interlayer polymeric phase between the carbon cloths, which was demonstrated by a decrease in standard deviations of the mean strength and modulus values. The results of the mechanical tests under dynamic bending loads indicated that ultrasonic wave propagation in the composite materials depended primarily on the elasticity of the carbon fibers themselves and their orientation to the propagation direction. The composite materials subjected to dynamic load amounting to  $10^6$  cycles retained their mechanical integrity when the maximum amplitude (deflection) of bending was 50% of the failure load. In the (2D) layered composites without CNTs a small increase in the standard deviation of dynamic elastic modulus was noted after the fatigue test.

The biological tests revealed that the viability of fibroblasts and osteoblasts determined in the MTT test after one week was slightly different from the control and the pure polymer. The value of viability was influenced by both the type of the material and the type of a cell line. Of the cells studied, osteoblasts displayed a higher survival level. The amount of collagen I produced by osteoblasts in contact with PEEK-based composites was higher than the amount of collagen I produced by these cells in the case of the control.

## Acknowledgements

The work has been supported by the Polish National Centre for Research and Development, project no N N507 463437 and by the Laryngology Department, School of Medicine, Medical University of Silesia in Katowice (Statute Found no: KNW-1-102/K/8/0 and no: KNW-1-043/K/7/0).




## ORCID iDs

W. Smółka:  <https://orcid.org/0000-0003-4074-9705>  
 M. Dworak:  <https://orcid.org/0000-0002-6962-9283>  
 M. Gubernat:  <https://orcid.org/0000-0002-5424-1091>  
 J. Markowski:  <https://orcid.org/0000-0003-3416-7354>  
 M. Błażewicz:  <https://orcid.org/0000-0001-9138-5409>

## References

- <http://onkologia.org.pl/nawotwory-zlosliwe-krtani-c32/>
- Lewin J.S., Baumgart L.M., Barrow M.P., Hutcheson K.A.: Device Life of the Tracheoesophageal Voice Prosthesis Revisited. *JAMA Otolaryngology- Head & Neck Surgery* 143(1) (2017) 65-71.
- van Sluis K.E., van der Molen L., van Son R.J.J.H., Hilgers F.J.M., Bhairosing P.A., van den Brekel M.W.M.: Objective and subjective voice outcomes after total laryngectomy: a systematic review. *European Archives of Oto-Rhino-Laryngology* 275(1) (2018) 11-26.
- Krishnamurthy A., Khwajamohiuddin S.: Analysis of Factors Affecting the Longevity of Voice Prosthesis Following Total Laryngectomy with a Review of Literature. *Indian Journal of Surgical Oncology* 9(1) (2018) 39-45.
- Choussy O., Hibon R., Bon Mardion N., Dehesdin D.: Management of voice prosthesis leakage with Blom-Singer large esophage and tracheal flange voice prostheses. *European Annals of Otorhinolaryngology, Head and Neck Diseases* 130(2) (2013) 49-53.
- Somogyi-Ganss E., Chambers M.S., Lewin J.S., Tarrand J.J., Hutcheson K.A.: Biofilm on the tracheoesophageal voice prosthesis: considerations for oral decontamination. *European Archives of Oto-Rhino-Laryngology* 274(1) (2017) 405-413.
- Monroe D.: Looking for chinks in the armor of bacterial biofilms. *PLoS Biology* 5(11) (2007).
- Kress P., Schäfer P., Schwerdtfeger F.P., Rösler S.: Are modern voice prostheses better? A lifetime comparison of 749 voice prostheses. *European Archives of Oto-Rhino-Laryngology*. 271(1) (2014) 133-40.
- <https://www.lmco.com/products/provox%20AE-vega%20AE-voice-prosthesis>
- Kurtz S.M., Devine J.N.: PEEK biomaterials in trauma, orthopedic, and spinal implants. *Biomaterials* 28(32) (2007) 4845-4869.
- Migacz K., Chlopek J., Morawska-Chochol A., Ambroziak M.: Gradient composite materials for artificial intervertebral discs. *Acta of Bioengineering and Biomechanics* 16(3) (2014) 4-12.
- Toth J.M., Wang M., Estes B.T., Scifert J.L., Seim H.B., Turner A.S.: Polyetheretherketone as a biomaterial for spinal applications. *Biomaterials* 27(3) (2006) 324-334.
- Xu A.X., Liu X.C., Gao X., Deng F., Deng Y., Wei S.C.: Enhancement of osteogenesis on micro/nano-topographical carbon fiber-reinforced polyetheretherketone-nanohydroxyapatite biocomposite. *Materials Science and Engineering: C* 48 (2015) 592-598.
- Hahnel S., Wieser A., Lang R., Rosentritt M.: Biofilm formation on the surface of modern implant abutment materials. *Clinical Oral Implants Research* 26(11) (2015) 1297-1301.
- Montero J.F., Tajiri H.A., Barra G.M., Fredel M.C., Benfatti C.A., Magini R.S., Pimenta A.L., Souza J.C.: Biofilm behavior on sulfonated poly(ether-ether-ketone) (sPEEK). *Materials Science and Engineering: C* 70(1) (2017) 456-460.
- Schwitalla A.D., Spintig T., Kallage I., Muller W.D.: Flexural behavior of PEEK materials for dental application. *Dental Materials* 31(11) (2015) 1377-1384.
- Brockett C.L., Carbone S., Abdelgaied A., Fisher J., Jennings L.M.: Influence of contact pressure, cross-shear and counterface material on wear of PEEK and CFR-PEEK for orthopaedic applications. *Journal of the Mechanical Behavior of Biomedical Materials* 63 (2016) 10-16.
- Nazimi A.J., Yusoff M.M., Nordin R., Nabil S.: Use of polyetheretherketone (PEEK) in orbital floor fracture reconstruction - A case for concern. *Journal of Oral and Maxillofacial Surgery, Medicine, and Pathology* 27(4) (2015) 536-539.
- Dworak M., Bloch M., Błażewicz S.: Chemical and mechanical study of PEEK/carbon fibre composite. *Engineering of Biomaterials* 69-72 (2007) 121-124.
- Dworak M., Rudawski A., Markowski J., Błażewicz S.: Dynamic mechanical properties of carbon fibre-reinforced PEEK composites in simulated body-fluid. *Composite Structures* 161 (2017) 428-434.
- Dworak M., Błażewicz S.: Mechanical assessment of a hip joint stem model made of a PEEK/carbon fibre composite under compression loading. *Acta of Bioengineering and Biomechanics* 18(2) (2016) 71-79.
- Meister K., Cobb A., Bentley G.: Treatment of painful articular cartilage defects of the patella by carbon-fibre implants. *Journal of Bone and Joint Surgery* 80 (1998) 965-970.
- Abarrategi A., Gutierrez M.C., Moreno-Vicente C., Hortiguela M.J., Ramos V., Lopez-Lacomba J.L.: Multiwall carbon nanotube scaffolds for tissue engineering purposes. *Biomaterials* 29 (2008) 94-102.
- Correa-Duarte M.A., Wagner N., Rojas-Chapana J., Morszczek C., Thie M., Giersig M.: Fabrication and Biocompatibility of Carbon Nanotube-Based 3D Networks as Scaffolds for Cell Seeding and Growth. *Nano Letters* 4 (11) (2004) 2233-2236.
- Magiera A., Markowski J., Menaszek E., Pilch J., Błażewicz S.: PLA-based hybrid and composite electrospun fibrous scaffolds as potential materials for tissue engineering. *Journal of Nanomaterials* (2017) 1-11.
- Seo K., Kim M., Kim D.H.: Candle-Based Process for Creating a Stable superhydrophobic surface. *Carbon* 68 (2014) 583-596.

# CHANGES OF STRUCTURE AND PROPERTIES OF PMMA-BASED BONE CEMENTS WITH HYDROXYAPATITE AFTER DEGRADATION PROCESS

ANNA LASKA-LEŚNIEWICZ<sup>1\*</sup> , MAŁGORZATA RACZYŃSKA<sup>1</sup>, MACIEJ WRÓTNIK<sup>2</sup> , ANNA SOBCZYK-GUZENDA<sup>1</sup> 

<sup>1</sup> LODZ UNIVERSITY OF TECHNOLOGY, DEPARTMENT OF MECHANICAL ENGINEERING, INSTITUTE OF MATERIALS SCIENCE AND ENGINEERING, 1/15 STEFANOWSKIEGO ST., 90-924 LODZ, POLAND

<sup>2</sup> DEPARTMENT AND HOSPITAL DEPARTMENT OF ORTHOPAEDICS, SILESIA MEDICAL UNIVERSITY, ST. BARBARA 5<sup>TH</sup> REGIONAL SPECIALISED HOSPITAL IN SOSNOWIEC,

PL. MEDYKÓW 1, 41-200 SOSNOWIEC, POLAND

\*E-MAIL: ANNA.LASKA.LESNIEWICZ@GMAIL.COM

## Abstract

*PMMA-based bone cements are commonly used for implant fixation or as bone void fillers. Hydroxyapatite added as a filler to bone cement may positively affect the final properties of the material, in particular its biological properties. In this study, the preparation of poly(methyl methacrylate)-based bone cements with incorporated hydroxyapatite (HAp) is reported. The purpose of this article is to examine the properties of bone cements enriched with HAp filler (the concentration of 3wt% and 6wt%) and reveal the changes in the composites properties (chemical structure, surface morphology and distribution of HAp in the composite matrix, moisture absorption, hardness in Shore D scale) during the long-term incubation in the PBS (phosphate-buffered saline) solution at 37°C. The incubation lasted up to 21 days, but only the period when the changes actually occurred was analysed. The studies have shown that the samples containing HAp absorb more moisture and have a lower hardness. These characteristics vary depending on the concentration of HAp. There is no elution of HAp and ZrO<sub>2</sub> from the composite during the incubation. The surface morphology and chemical structure do not change during long-term studies. The obtained bone cements are characterized by high stability in the PBS solution.*

**Keywords:** bone cement, PMMA, hydroxyapatite, vertebroplasty

[*Engineering of Biomaterials* 151 (2019) 9-16]

## Introduction

Bone cements have been widely used in medicine since the 1960s when joint replacements started to be common orthopaedic surgical procedures. The significant increase in physical activity among people over 50 years of age, a higher rate of obesity in the population, ageing of the population and perpetual rise of patients' demands combined with development of new implants used in treatment of osteoarthritis will result in a rise of numbers of joint replacements in next decades.

According to the latest data, osteoarthritis (OA) affects 240 million people globally, about 10% of men and 18% of women over 60 years of age [1]. There are both conservative and surgical methods of OA treatment, however the first one is still ineffective and cannot stop the OA progression. Therefore, the total joint replacement is the most successful method of osteoarthritis treatment reducing pain and improving the quality of life. The total hip replacement arthroplasty (THA) and total or uni-compartment knee arthroplasty (TKA, UKA) are the most common procedures in the everyday practice of orthopaedic surgeons. In both cases, the bone cement is to fasten the joint endoprosthesis. The final result of the treatment depends on a properly selected implant, accordingly to the patient's age, bone quality and future activity, their demands and expectations and indications for the operation. Therefore, selecting biomaterials that will provide the efficient and long-lasting stability of the implant is yet another aspect. In patients with osteoporosis, whose bone tissue is less resistant to physical stress, fixing bone cement is the most important factor that influences the implant lifespan and may provoke its early loosening.

Among other applications, bone cements are implemented to fill up minor bone cavities mainly in the facial area. They are also used in other medical procedures, such as vertebroplasty (VP) and kyphoplasty (KP) – that are preferred methods of treating stable, compression fractures of vertebral body. This type of vertebral fractures, combined with fractures of the proximal humerus and femoral neck, are the most frequent injuries in patients with osteoporosis. Both VP and KP are minimally invasive and designed mainly to relieve the pain, strengthen collapsed vertebrae and finally restore geometry of the vertebral column [2]. Furthermore, VP is a palliative method of treatment in pathological spinal fractures in the case of metastases of the vertebral column [3]. As the population in Europe is ageing and the statistics shows progressive osteoporosis, increased spinal fractures and joint problems, the development of such biomaterials as bone cements that will fully meet the requirements of bone rebuilding and bonding the implant with tissue seems to be inevitable [4].

Bone cements can be divided due to the materials they were made of. There are polymeric, phosphate-calcium-based, hydrogel and composite bone cements [5]. The most popular ones are cements based on poly(methyl methacrylate) (PMMA). They have long clinical history, therefore it is easier to predict their behaviour in the human body over the years. The PMMA cement exhibits biocompatibility and appropriate mechanical properties. Still, it is possible to develop composites so that the connection between the injected cement and surrounding tissue will improve. That is why bioactive bone cements with the addition of bioactive glass or hydroxyapatite are a particularly promising solution [6,7].

Requirements for bone cements are strictly related to their use. In the case of fixing endoprostheses, cement can form just a mechanical connection with the bone (without chemical bonding). According to the ISO norm (ISO 5833), its compressive strength must be higher than 70 MPa. For the bone defect reconstruction or filling, cements should also exhibit osteoconductive effects and support tissue regeneration. The material introduced into bone defects may be characterized by lower strength parameters, similar to the properties of natural spongy bone tissue (at least 30 MPa). PMMA-based cements are endowed with good mechanical properties (Young's modulus – 1800-2200 MPa, compressive strength – 75-105 MPa, bending strength – 60-75 MPa) and the ease of feeding resulting from good rheological properties [8,9].

In addition, the rheological properties of cement, its setting time and behaviour in contact with the physiological fluid are important. The chemical and granular composition has a significant impact on these parameters. The widespread use of bone cements in orthopaedics and facial-jaw surgery forces their modifications which will improve their biological and mechanical properties.

Polymeric cements are two-component systems – powder and liquid, whose weight ratio is about 2:1. The powder usually consists of poly(methyl methacrylate) (PMMA) or a copolymer of styrene and methyl methacrylate. In addition, a polymerization initiator – benzoyl peroxide and radiopaque agents – barium sulphate or zirconium dioxide are added. The liquid contains methyl methacrylate monomer (MMA), about 98% by weight. Additionally, bone cements may contain antibiotics, e.g. gentamicin or vancomycin, which increases the septicity of the medical procedure [10].

Unfortunately, PMMA cements are also burdened with negative effects on the human body. The biggest problems associated with their use include:

- exothermic reaction related to the mechanism of polymerization of this material,
- polymerization shrinkage,
- poor adhesion to the bone surface and inorganic substance,
- lower resistance to cracking (compared to natural bone),
- leaving 4-7% unreacted MMA monomers with toxic effects.

Composite bone cements are the answer to problems occurring mainly with PMMA-based cements. The selection of the reinforcement phase plays a key role for the strength and stability of the bone cement in the human body. The contribution of reinforcement (a filler) in the composites equals usually from a few to several percent by weight. Changes in material properties may be noted even after minor addition of a filler (such as 1%wt) but there is no obvious correlation that can be simply stated about all reinforcement types. In the case of such fillers as bovine bone pulp, bone-substitute material and  $Al_2O_3$ , the significant changes in mechanical properties and the polymerisation course are found in samples with a filler quantity of more than 5% [11]. What is more, the type and amount of a filler determines the polymerization course, the material solidification and its behaviour in contact with the tissue. The addition of bioactive glass, hydroxyapatite or calcium triphosphate results in a decrease in compressive properties (slight deterioration of strength properties), it reduces porosity and improves fracture toughness. Composites containing starch are characterized by better degradation and resorbability [12].

Hydroxyapatite (HAp) –  $Ca_{10}(PO_4)_6(OH)_2$  naturally occurs in human bones. It is slightly soluble in water and resilient in tissues, therefore it facilitates the integration of tissues and bone restoration. The introduction of hydroxyapatite into the polymer phase may increase biocompatibility and facilitate performing biomechanical functions. Additionally, bioactive HAp particles can act as anchors for the composite - bone bonds, which ensures good restoration of the living tissue and promotes bone growth around the implant [13]. Moreover, according to the research, the bone cement based on poly(methyl methacrylate-co-styrene) filled with HAp has a lower exothermic effect during the curing process and a higher degree of conversion (which means a lower residual monomer amount) than the cement without this addition [14,15]. The HAp addition also influences the mechanical properties of bone cement, but it is hard to clearly estimate the trend.

The aim of the present study was to describe and characterise the novel composite bone cements in terms of the chemical composition and structure, surface morphology, moisture uptake and changes in hardness over different time of incubation in a buffer at 37°C. The new materials described in this work are based on the commercial PMMA bone cement loaded with a biocompatible and bioactive hydroxyapatite powder (HAp) that was precisely selected and synthesised.

## Materials and Methods

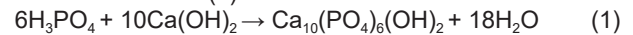
### Materials

Commercial bone cement is used as a polymeric matrix of the tested samples. The chemical composition of bone cement (BC) is presented in TABLE 1.

**TABLE 1. Chemical composition of commercial basic bone cement.**

Powder phase (26 g)	Poly(methyl acrylate, methyl methacrylate)
	Zirconium dioxide
	Benzoyl peroxide
	Colouring agent E141 – Chlorophyll
Liquid phase (10 ml)	Methyl methacrylate
	N, N-dimethyl-p-toluidine
	Hydroquinone

Hydroxyapatite powder, a filler in the created bone cement, was synthesized via the chemical wet method i.e. precipitation. The process was based on the experiments carried out by Afshar and co-workers [16] via the following chemical reaction (1):



As it was calculated, for the synthesis approx. 50 g of powdered HAp and 37 g of calcium hydroxide ( $Ca(OH)_2$ , Chempur) was added to 4 liters of distilled water and mixed for 1 hour at 40°C ( $\pm 2^\circ C$ ). Then, 34.6 g of orthophosphoric acid ( $H_3PO_4$ , POCH) was gradually poured into the mixture at the speed of 1 drop per second. At that stage, it was crucial to control the temperature ( $40 \pm 2^\circ C$ ) and the pH value (above 9). If pH came closer to 9, a small amount (10 ml) of ammonia solution 25% (POCH) was added. After the synthesis, the sediment was purified at least 10 times in order to get rid of the ammonia solution. Then, the synthesized HAp was dried at room temperature. Final steps were milling and sifting (screening). The material was milled in the planetary ball mill (Retsch, Germany) and sieved in the laboratory sifter (Morek Multiserw, Poland) to get the proper particle size of 25-50  $\mu m$ .

Dulbecco's phosphate-buffered saline (PBS, Corning Media) without calcium and magnesium was used to immerse all the bone cement samples for the experiments.

### Preparation of bone cements

The three types of specimens were prepared for examinations: (1) the control sample – the commercial bone cement without hydroxyapatite (Osteopal® plus), (2) the 3%HAp/BC - the commercial bone cement with 3wt% HAp, (3) the 6%HAp/BC - the commercial bone cement with 6wt% HAp. The composition of all specimens is presented in TABLE 2.

TABLE 2. Composition of specimens.

Sample name	Powder phase		Liquid phase	Powder/Liquid Ratio
	Bone Cement	HAp		
Control sample (Bone Cement – BC)	3 g	-	1.154 ml	2,6
3%HAp/BC	3 g	0.126 g	1.154 ml	2,7
6%HAp/BC	3 g	0.261 g	1.154 ml	2,83

The novel bone cements were prepared in three steps. Firstly, the powder phase of the commercial bone cement was precisely mixed with synthesised HAp powder in proper amounts. Then, the new powder phase was manually mixed, using a spatula, with the liquid in a small glass beaker for 30–40 s at room temperature. Finally, the material was transferred into silicon moulds. The samples were prepared as cylinders of measuring 6 mm or 12 mm in diameter and 2 mm in height.

### Degradation test

Three types of specimens (the control sample BC, the 3%HAp/BC, the 6%HAp/BC) were subjected to degradation tests. The samples (cylindrical shape,  $\phi$ 6 mm) were soaked in the PBS buffer and kept in an incubator at 37°C for different periods of immersion. i.e. 7 days, 21 days, 42 days. After the incubation, the samples were preliminarily dried with a paper towel and then left at room temperature. The incubated specimens were tested, using the following techniques:

- Scanning Electron Microscope (SEM) – morphology of the sample surfaces,
- Energy Dispersive X-ray Spectroscopy (EDS) – elemental composition and maps of the distribution of elements,
- Fourier Transform Infrared Spectroscopy (FTIR) – chemical structure,
- Shore D hardness test after 7 and 21 days of incubation,
- Moisture uptake after 7-day, 21-day and 42-day immersion in the buffer.

### Morphology of the bone cements

The surface morphology of the composite bone cements was examined on the JSM-6610LV Scanning Electron Microscope (SEM, JEOL USA). The samples were observed right after preparation (before the incubation) and after being soaked in PBS for 21 days. To obtain clear images the samples were covered in a thin (10 nm) layer of gold. The detailed images of two different magnifications (x100 and x1000) were obtained under high vacuum and at 20 kV accelerating voltages.

### Elemental composition of bone cements

The composition of the cements was confirmed via EDS. The additional module X-MAX 80 (Oxford Instruments) attached to the JEOL JSM-6610LV scanning electron microscope was used for the EDS X-ray microanalysis. The 20 kV acceleration voltage was used for the measurements. The scanning time of 7 min, the resolution of 2048 px and the excitation time of 100  $\mu$ s/px were set for the measurements. The maps of the distribution of selected elements were made.

### Chemical structure

For studies of the chemical structure of the samples, the Nicolet IS 50 FT-IR Spectrophotometer (FTIR, ThermoScientific) was used. The system was equipped with deuterated tri-glycine sulphate (DTGS) KBr beam splitter. The special reflection attachment (DRIFT type) with the incidence angle of 90° was used for the measurements. The FTIR spectra of absorbance over the wavelength range of 4000–400  $\text{cm}^{-1}$  with the resolution of 4  $\text{cm}^{-1}$  were measured.

### Hardness test

The indentation hardness of the specimens was determined by means of the durometer (Shore hardness scale D) according to the norm ISO 868:2003. The tests were conducted using the manual durometer MC-DX/D (max: control measuring instruments). Ten independent measurements were taken for each sample. The samples were tested before the immersion in PBS and after the immersion of 7 and 21 days.

### Moisture uptake

The cement samples (small cylinders of 6 mm in diameter and height of approx. 3 mm) were soaked in PBS at 37°C, up to 42 days. The moisture uptake (MU) was calculated according to the equation: (1) [12].

$$\text{MU} = [(m_i - m_0)/m_0] \times 100 \quad (1)$$

$m_0$  – initial mass (before immersion)

$m_i$  – sample mass after  $i$  immersion days.

## Results and Discussions

The morphologies of the studied bone cements are presented in FIG. 1. At the x100 magnification, there are no significant differences between the samples with varied HAp additions and the control sample (the bone cement without HAp). In the samples containing hydroxyapatite there are small white particles visible in the pictures (FIG. 1B and FIG. 1C). The morphologies, investigated at the low magnification, confirm the non-defected structure in all the specimens. Therefore, it can be deduced that the HAp addition does not adversely affect the material structure and the bone cements preparation proceeds correctly.

There are three characteristic structures visible in the images presented in FIG. 2: zirconium dioxide  $\text{ZrO}_2$ , PMMA and HAp.  $\text{ZrO}_2$  creates the bright, sizeable, cauliflower structures. PMMA can be recognised as spherical, bubble-like and dark-grey grains. HAp is noticeable as tiny irregular shapes, bright shreds on the surface. It is worth recalling that both zirconium dioxide and HAp act as fillers in the created bone cements. Their regular distribution and degree of fineness have a strong impact on the mechanical properties of the composite. The content of zirconium dioxide in the composite is 40wt%, which is many times more than the HAp amount. It is also clearly visible that the amount of zirconium is higher than HAp (even considering 6%HAp specimen). What is more, the zirconium tendency to agglomerate is observed. The size of the zirconium dioxide agglomerates was estimated to be of 20–30  $\mu\text{m}$  and is significantly larger than HAp grains (about 1–2  $\mu\text{m}$ ). It cannot be unequivocally stated that any of the components eluted during the incubation. The comparison of the morphology before and after the immersion does not reveal any visible changes.

The distribution of such elements as zirconium, calcium and phosphate is illustrated in the maps (FIG. 3). The control sample contains only zirconium, there are no maps for Ca and P, as it does not contain HAp. The maps of the 3%HAp/BC and the 6%HAp/BC confirm the occurrence of hydroxyapatite in their structures. In all the specimens, Zr, Ca and P show the tendency to agglomerate, they create clusters that are quite unevenly distributed in the material.



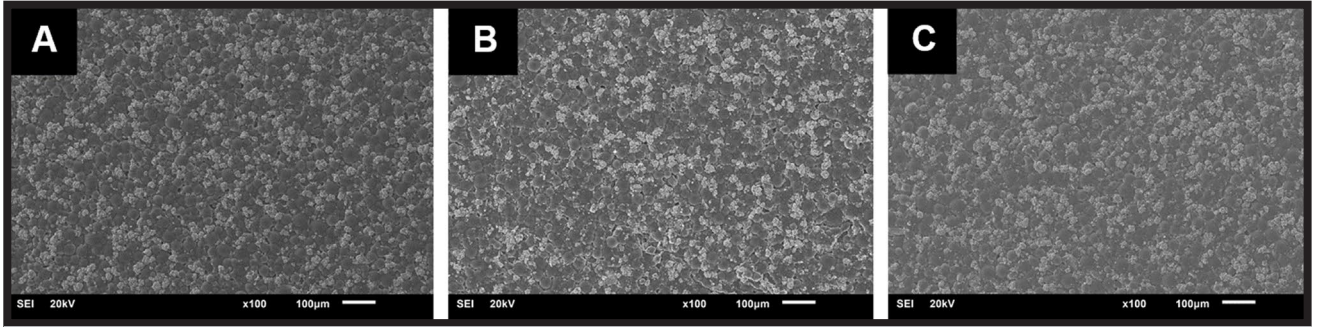


FIG. 1. Morphology of the prepared bone cements (A – control BC sample, B – 3%HAp/BC, C – 6%HAp/BC).

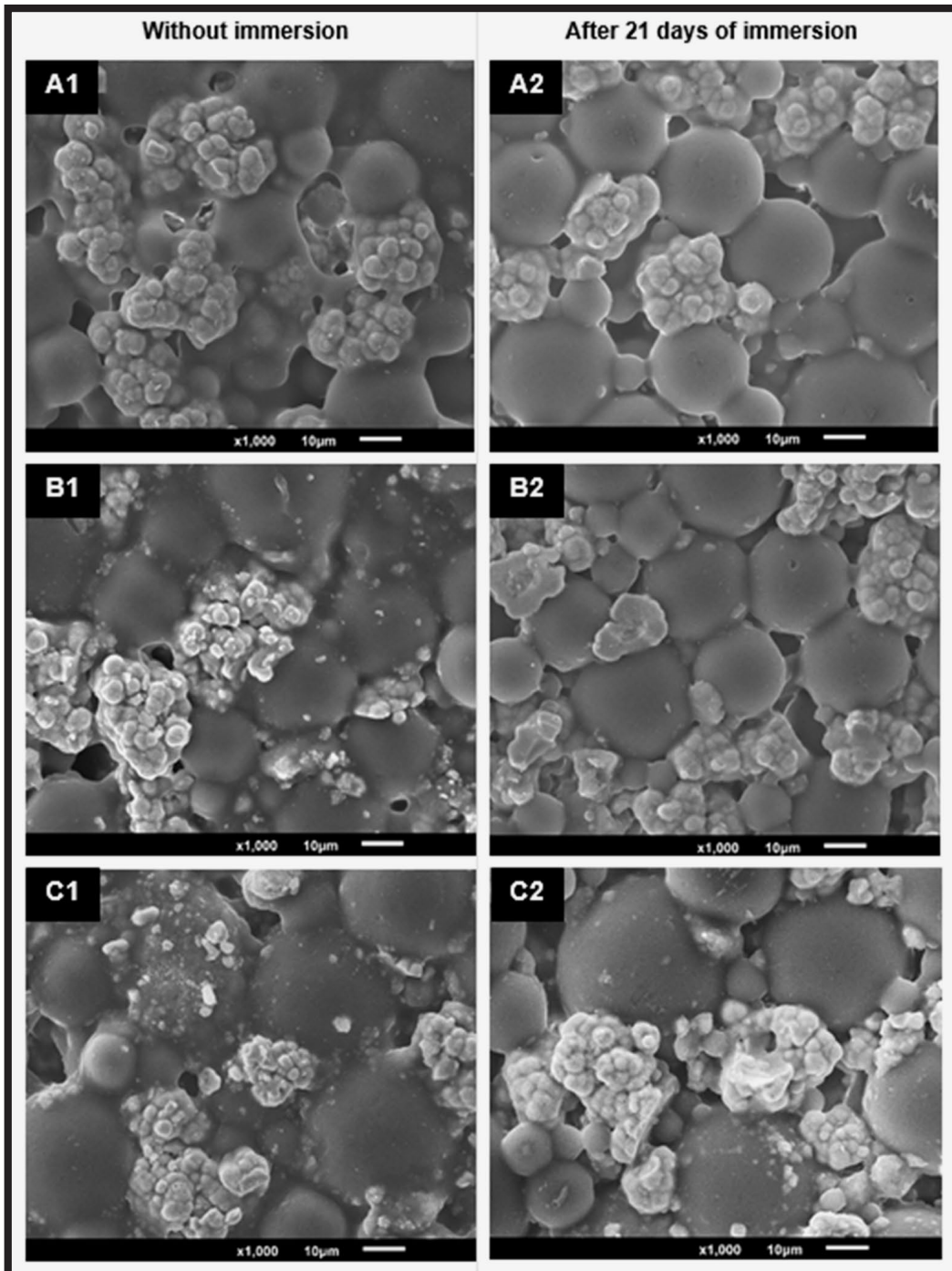


FIG. 2. SEM images before and after immersion in PBS (A1 – control BC sample before immersion, A2 – control BC sample after immersion; B1/ B2 – 3%HAp/BC before/after immersion; C1/C2 – 6%HAp/BC before/after immersion).

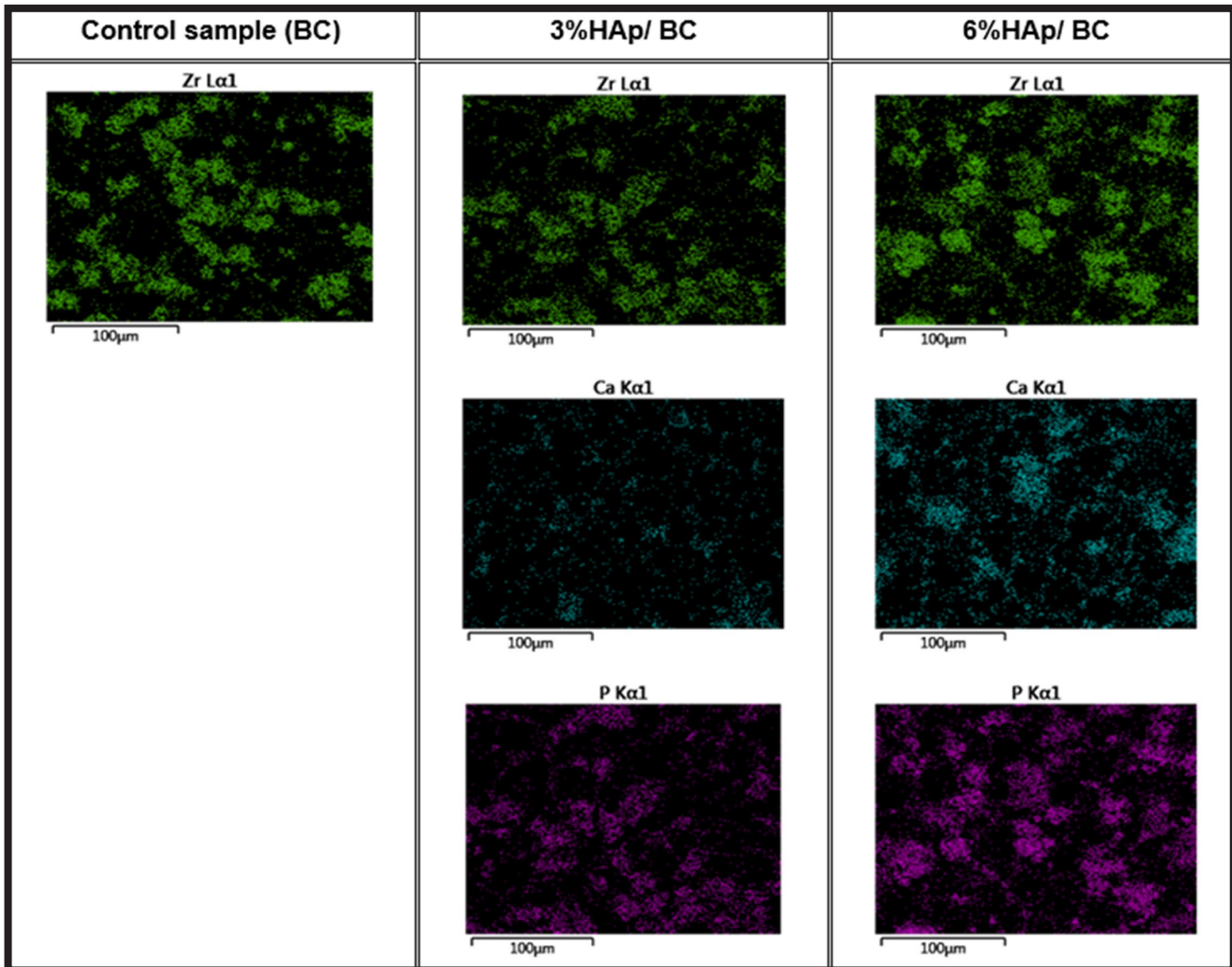


FIG. 3. Maps of the distribution of zirconium, calcium and phosphate in all tested samples.

The maps were also prepared after the 21-day immersion in the PBS solution. There was no visible elution of either HAp or zirconium dioxide over time. In FIG. 4 there are visible agglomerates of calcium. The tendency to agglomerate increases with the higher content of HAp. After the incubation the amount of calcium noticeably rises over 1wt% in both the sample types (3%HAp/BC and 6%HAp/BC).

FIG. 5A depicts the FTIR spectra for the bone cement samples. Based on the spectra, it can be concluded that a minor HAp addition slightly affects the chemical structure of the material.

As expected, the collected FTIR spectra display peaks characteristic for the bone cements based on poly(methyl methacrylate) (FIG. 5). The most prominent peaks occur at  $1729\text{ cm}^{-1}$  and from  $2750$  to  $3000\text{ cm}^{-1}$  corresponding to C=O stretch and  $-\text{CH}_2$ ,  $-\text{CH}_3$  stretch, respectively. The peak at  $3000\text{ cm}^{-1}$  decreases with the rising amount of HAp in the samples.

The characteristic peaks for Zr-O at  $750$ ,  $610$  and  $430\text{ cm}^{-1}$  are visible in all the spectra, which confirms the presence of that kind of a radiopacifier agent.

For the 3%HAp/BC and the 6%HAp/BC spectra the wide and visible peak at  $857\text{ cm}^{-1}$  can be attributed to ions  $\text{HPO}_4^{2-}$  present in HAp. The peak rises substantially with the increasing HAp content. Another peak at  $1083\text{ cm}^{-1}$  changes similarly. It represents ions  $\text{PO}_4^{3-}$  present in HAp.

The peak at  $565\text{ cm}^{-1}$  is generated by benzene rings and the other three bands come from the O-H bond in alcohols and phenols. Such groups are present in compounds that regulate the initiation and kinetics of polymerization (benzoyl peroxide, hydroquinone, N, N-dimethyl-p-toluidine). These substances are not inert to living organisms and their amount should be vestigial. All the visible differences are related to the chemical composition of the prepared bone cements and changes in the HAp/polymeric matrix ratio.

The peak at the wavelength of  $716\text{ cm}^{-1}$  is visible in each spectrum, but it is slightly wider and less pointy in the 6%HAp. It is connected with the Ar-OH bond in phenols (present in the hydroquinone structure). The mentioned change is related to another peak (at the wavelength of  $716\text{ cm}^{-1}$ , generated by  $\text{P}_2\text{O}_7^{4-}$ ) that merges with it. It seems that, as a result of the HAp precipitation, the trace amount of other ions was noted (absent in the HAp structure).

The peak at the wavelength of  $1012\text{ cm}^{-1}$  which decreases with the increasing HAp amount represents the C-O bonds in esters.

The minor, slightly visible peak at the wavelength of  $565\text{ cm}^{-1}$  and more visible peaks at  $3629$ ,  $3830$ ,  $3946\text{ cm}^{-1}$  slightly decrease with the increasing HAp content and are less visible in the 6% specimen spectra. The peak at  $565\text{ cm}^{-1}$  is generated by benzene rings and the other three bands come from the O-H bonds in alcohols and phenols. Such groups are present in the compounds that regulate the initiation and kinetics of polymerization (benzoyl peroxide, hydroquinone, N, N-dimethyl-p-toluidine). These substances are not neutral to living organisms and their amount should be limited.

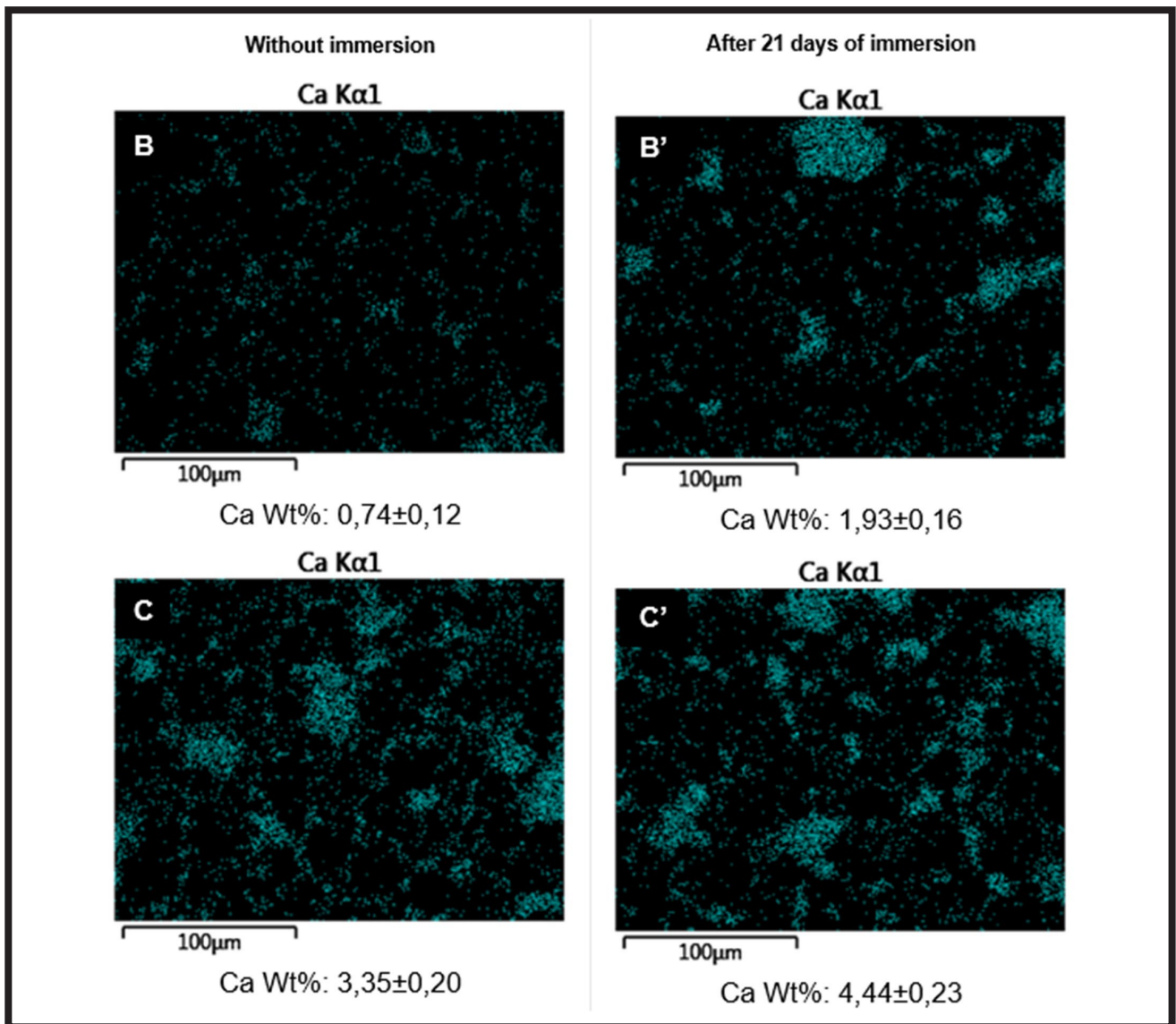


FIG. 4. Maps of calcium distribution before and after immersion in PBS (A1 – 3% HAp/BC before immersion, A2 – 3% HAp/BC after immersion, B1 – 6% HAp/BC before immersion, B2 – 6% HAp/BC after immersion).

FIGs 5B-5D show the spectra of all the types of bone cements after different immersion time. The analysis of the control sample spectra (bone cement) does not reveal any significant changes. In contrast, the spectra of the samples containing HAp display clearly visible changes.

The trend of the observed changes cannot be unambiguously determined. Non-schematic changes in peak values that represent bonds in HAp and polymeric bone cement matrix are most likely related to minor changes in the composition and the HAp distribution in heterogeneous samples.

Before the incubation, the highest hardness value was noticed for the control sample – the bone cement without hydroxyapatite (FIG. 6). The higher amount of HAp was the lower hardness. The differences in hardness between the bone cements with HAp are slight. After the incubation there were some changes in the hardness values. In general, the storage in PBS worsens the samples hardness. Those changes may be partly connected with the moisture uptake of the bone cements. Small molecules of water absorbed into the bone cement between the long chains of poly(methyl methacrylate) act as a “plasticizer” of the polymer structure. Most probably, the addition of a ceramic filler such as HAp increases the inhomogeneity and influences the mechanical properties of the composites.

The moisture uptake results (FIG. 7) show that the cement is getting filled by liquid most at the beginning of the immersion, regardless of its composition. The tests indicate that the largest increase in mass, i.e. the greatest moisture uptake at that time, which is coherent with the literature [12,17]. The amount of the absorbed solution gradually decreases over time. However, another process should be taken into consideration that has an impact on the specimen mass – the release of residual monomer. Since the PMMA matrix is hydrophobic, it is possible that the mass values of the absorbed moisture and the released monomer are comparable. One can assume that the released monomer amount is higher than the absorbed moisture weight. The weight changes vary, depending on the HAp content. The 6% HAp weight increased twice as much as the control sample on the 7th day of measurement. The 3% HAp weight grew one and a half times more than the control. The most significant change in weight was recorded for the specimens with HAp, this phenomenon is related to the heterogeneous structure of the composite with the highest value of a ceramic filler. Water easily penetrates a porous, heterogeneous structure with the well-developed area of the phases boundary between the PMMA matrix and the filler. The more numerous the heterogeneities are, the more spaces where water can be accumulated.

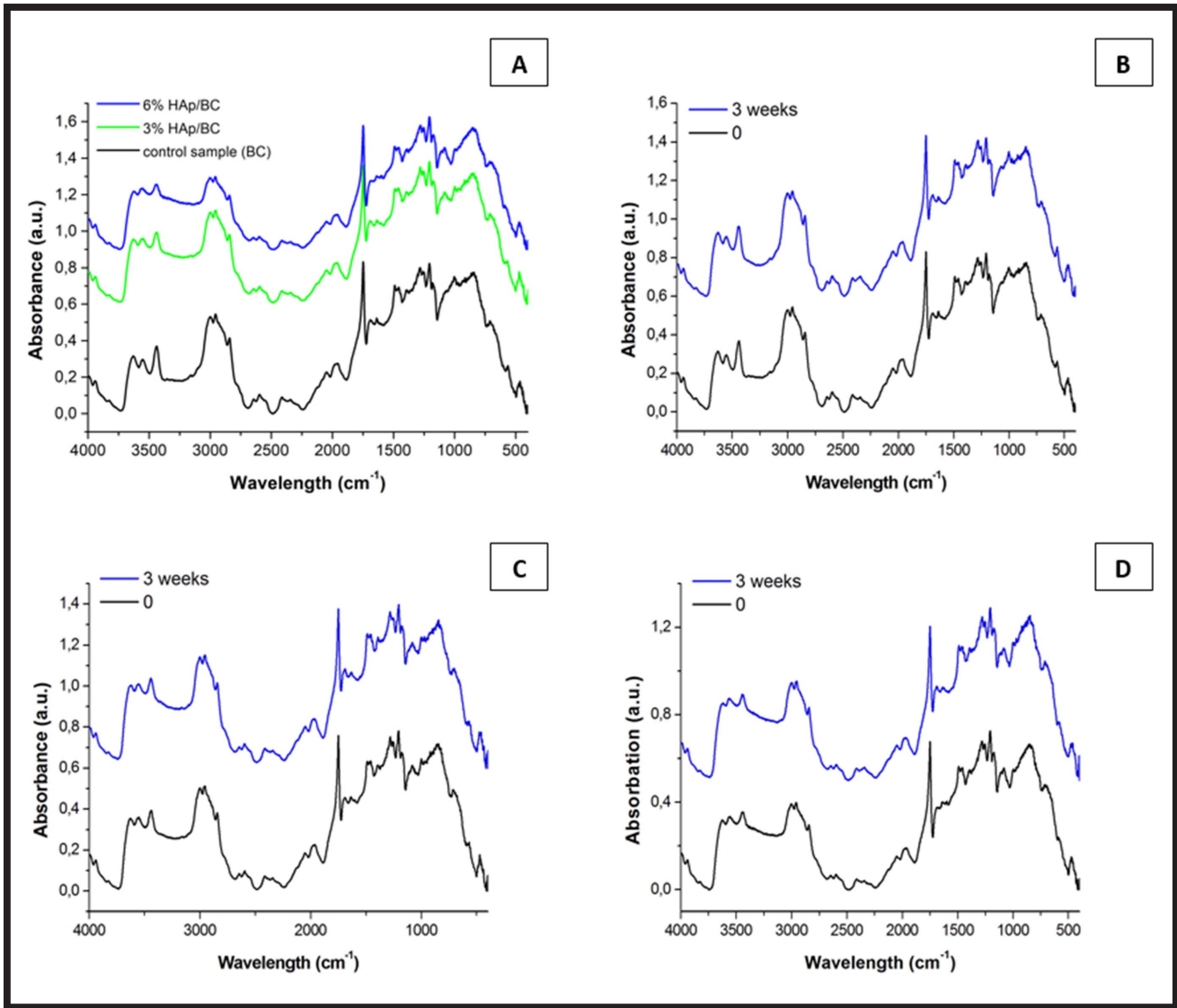


FIG. 5. FTIR spectra (A – spectra of all prepared samples before immersion, B – spectra of control sample over immersion time, C – spectra of 3% HAp/BC over immersion time, D – spectra of 6% HAp/BC over immersion time).

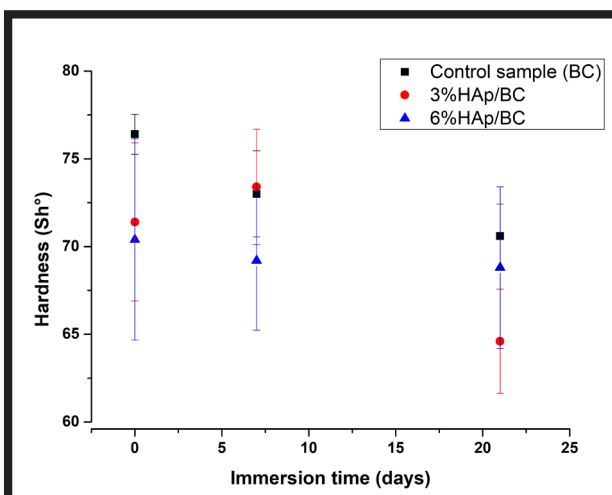


FIG. 6. Changes in hardness (Shore D scale) after immersion in PBS buffer.

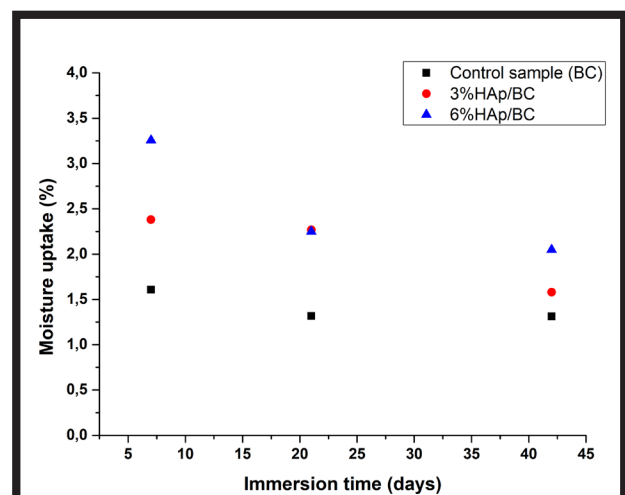


FIG. 7. Moisture uptake over different immersion time.

## Conclusions

Hydroxyapatite is a ceramic filler that can be used in polymer-based bone cements. It may improve poor biological properties of those biomaterials, especially by enhancing osseointegration between the living bone and an artificial implant.

The morphology and the chemical structure of the prepared samples – the bone cements without and with hydroxyapatite have insignificantly changed over time of the PBS incubation. However, the amount of calcium increased under the liquid conditions. After the FTIR analysis, it may be concluded that there are no big differences in the position or magnitude of intensity peaks after the samples immersion, indicating that hardly any new chemical groups were formed. The chemical structure analysis revealed unexpected features of precipitated HAp. Despite the strict compliance with the procedure, additional phosphate ions were observed. The SEM images and the maps of the sample composition draw attention to another issue. The ceramic filler (HAp) is significantly less finely divided than zirconium dioxide ( $ZrO_2$ ). This feature may affect the properties of the entire bone cement. However, HAp is distributed more evenly and has a smaller tendency to agglomerate than  $ZrO_2$ . Unfortunately, it is also noticeable that the most common location of HAp is in the phases boundary and the HAp adhesion to other compounds is weak.

The PMMA-based bone cements also undergo changes in mechanical properties during the incubation. The extent of these changes can be attributed to the moisture uptake, the cement composition and the immersion time. A typical change is an increase in the sample mass. Regarding the moisture absorption test, it can be estimated that the HAp addition enhances the moisture absorption, which may affect the material structure, worsen the mechanical properties and accelerate the cement degradation in the future.

Exact changes are difficult to assess due to the simultaneous occurrence of another process affecting mass – the release of residual monomer (MMA) into the solution.

The differences in hardness are not enormous but these changes are problematic in time. This factor influences the growth of adjacent bone tissue and variable mechanical properties of the material may lead to the implant loosening in the human body. Therefore, taking into account the rapidity of these changes, the sample filled with a large amount of the filler (6% HAp and 3% HAp) seem to be the best solution.

What is more, too high concentration of the HAp filler may worsen the injectability, which is a crucial factor for medical applications. Since the results of the study indicated changes in the polymerization process depending on the HAp content, the appropriate selection of components that regulate the kinetics, course and initiation of this reaction is also worth considering.

## Acknowledgement

*This work was performed within the framework of funding of Lodz University of Technology, Institute of Materials Science and Engineering.*

## ORCID iDs

A. Laska-Leśniewicz:  <https://orcid.org/0000-0002-0546-0378>






M. Wrotniak:  <https://orcid.org/0000-0002-4329-8623>

A. Sobczyk-Guzenda:  <https://orcid.org/0000-0003-1583-4238>

## References

- [1] A.E. Nelson: Osteoarthritis year in review 2017: clinical, Osteoarthritis and Cartilage 26 (2018) 319-325.
- [2] C. Robo, C. Ohman-Magi, C. Persson: Compressive fatigue properties of commercially available standard and low-modulus acrylic bone cements intended for vertebroplasty. J. Mech. Behav. Biomed. Mater. 82 (2018) 70-76.
- [3] A. Delpla, L. Tselikas, T. De Baere, S. Laurent, K. Mezaib, M. Barat, O. Nguimbous, C. Prudhomme, M. Al-Hamar, B. Moulin, F. Deschamps: Preventive Vertebroplasty for Long-Term Consolidation of Vertebral Metastases, Cardiovasc Intervent Radiol 42(12) (2019) 1726-1737.
- [4] E. Herlund, A. Svedbom, M. Ivergård et al.: Osteoporosis in the European Union: medical management, epidemiology and economic burden. Arch Osteoporos. 8(1-2) (2013) 136.
- [5] A. Balin: Cementy w chirurgii kostnej, Wyd. Politechniki Śląskiej (2016) 13-23.
- [6] J. Łukaszczyk: Polimerowe i kompozytowe cementy kostne oraz materiały pokrewne, cz. I. Klasyczne cementy metakrylanowe i ich modyfikacja. Polimery 49(2) (2004) 79-88.
- [7] J. Łukaszczyk, M. Śmiga-Matuszowicz: Polimerowe i kompozytowe cementy kostne oraz materiały pokrewne, cz. II. Kompozyty resorbowalne i wykazujące aktywność biologiczną. Polimery 55(2) (2010) 83-92.
- [8] A. Boger, K. Wheeler, B. Schenk: Clinical investigations of poly(methyl methacrylate) cement viscosity during vertebroplasty and related in vitro measurements. Eur Spine J 18 (2009) 1272-1278.
- [9] M. Jayabalan, K. Shalumon, M. Mitha: Injectable biomaterials for minimally invasive orthopaedic treatments. J Mater Sci: Mater Med 20 (2009) 1379-1387.
- [10] W. Jiranek, A. Hanssen, A. Greenwald: Antibiotic – loaded bone cement for infection prophylaxis in total joint replacement. J. Bone Joint Surg. Am 88 (2006) 2487-2500.
- [11] J. Włodarski: Wpływ wypełniaczy na właściwości wytrzymałościowe kompozytowych cementów kostnych. Kompozyty 5 (2005) 78-82.
- [12] C. Aubrun-Fillatre, F. Monchau, P. Hivart: Acrylic bone cement and starch: botanical variety impact on curing parameters and degradability. Material Science and Engineering C 69 (2016) 1328-1334.
- [13] A. Sobczak, Z. Kowalski: Materiały hydroksyapatytowe stosowane w implantologii. Czasopismo Techniczne. Chemia 104 (1) (2007) 149-158.
- [14] L. Morejón, J.A. Delgado, N. Davidenko, E. Mendizábal, E.H. Barbosa, C.F. Jasso: Kinetic effect of hydroxyapatite types on the polymerization of acrylic bone cements. International Journal of Polymeric Materials and Polymeric Biomaterials 52(7) (2010) 637-654.
- [15] L. Morejón, A.E. Mendizábal, et al.: Static mechanical properties of hydroxyapatite (HA) powder-filled acrylic bone cements: Effect of type of HA powder. J. Biomed. Mater. Res. B Appl. Biomater. 15, 72(2) (2005) 345-352.
- [16] A. Afshar, M. Ghorbani, N. Ehsani, et al.: Some important factors in the wet precipitation process of hydroxyapatite. Materials and Design 24 (2003) 197-202.
- [17] W.N. Ayre, S.P. Denyer, S.L. Evans: Ageing and moisture uptake in polymethyl methacrylate (PMMA) bone cements. J. Mech. Behav. Biomed. Mater. 32 (2014) 76-88.

# SURFACE MODIFICATIONS FOR INFLOW CANNULAS OF VENTRICULAR ASSIST DEVICES – COMPARISON OF LATEST SOLUTIONS

PRZEMYSŁAW KURTYKA<sup>1,2\*</sup> , ROMAN KUSTOSZ<sup>1</sup> ,  
MARCIN KACZMAREK<sup>2</sup> , MAŁGORZATA GONSIOR<sup>1</sup> ,  
KLAUDIA TOKARSKA<sup>3</sup> 

<sup>1</sup> FOUNDATION OF CARDIAC SURGERY DEVELOPMENT, ARTIFICIAL HEART LABORATORY, UL. WOLNOŚCI 345A, 41-800 ZABRZE, POLAND

<sup>2</sup> DEPARTMENT OF BIOMATERIALS AND MEDICAL DEVICES ENGINEERING, FACULTY OF BIOMEDICAL ENGINEERING, SILESIA UNIVERSITY OF TECHNOLOGY, UL. ROOSVELTA 40, 41-800 ZABRZE, POLAND

<sup>3</sup> CENTRE OF POLYMER AND CARBON MATERIALS, POLISH ACADEMY OF SCIENCES (CMPW PAN), UL. M. CURIE-SKŁODOWSKIEJ 34, 41-819 ZABRZE, POLAND

\*E-MAIL: PKURTYKA@FRK.PL

## Abstract

*Nowadays, the Mechanical Circulatory Support (MCS) within the Ventricular Assist Devices (VAD) appears to be a reliable and effective solution for patients with advanced heart failure (HF). After many years of work, extracorporeal pulsatile VADs have been replaced by new generations of implantable continuous flow (CF) pumps. Clinical experience has shown that present-day pump constructions still need to be improved to minimize the risk of complications during heart assistance.*

*One of the complications is the pump inflow obstruction caused by the ingrowth of tissue into the blood inflow path and pump thrombosis. The main goal is to develop a coating for the external surface of the inflow cannula to provide controlled tissue ingrowth. The smooth surface of the cannula external wall results in the tissue overgrowth into the pump inflow orifice, and may be a source of emboli. The paper presents external surface modifications of the inflow cannula performed by different VAD manufacturers within the topography characterization.*

*The inflow cannulas used in CF VADs are mainly made of titanium alloy due to its mechanical properties and high biocompatibility. In general, the discussed surface coatings were characterized by the roughness of about  $\approx Ra = 15 \mu m$ , high porosity and good wettability  $\Phi \approx 60^\circ$ . The surface was covered with titanium microspheres or titanium mesh.*

*The developed surfaces and clinical experience confirm the ability to control the tissue ingrowth along the external surfaces of the inflow cannula at the tissue-implant interface.*

**Keywords:** surface modification, VAD inflow cannula, tissue-implant interface, porous surface

[Engineering of Biomaterials 151 (2019) 17-23]

## Introduction

Surface modifications of medical implants provide many possibilities to control the processes occurring after implantation in peri-implant tissues. The healing process of orthopaedic implants and the processes occurring in bone tissues after implantation have already been well described in the literature and the provided knowledge is successfully used in the clinic. An example is the modification of surfaces in cementless endoprostheses where the surface coating increases the potential for biomechanical bonding at the implant-bone interface and affects the rate of protein adsorption [1-5]. A close correlation between pore size and bone ingrowth is also noticeable [5-7]. Unfortunately, there is still no data concerning issues of cardiac surgical implants healing, despite the widespread use of mechanical circulatory support systems. Therefore, it is necessary to provide clinical data which will determine the morphological parameters of the surface coating providing a permanent and stable connection of cardiac implants with myocardial tissue.

Nowadays, the Mechanical Circulatory Support (MCS) is becoming a viable alternative to heart transplantation for non-effective pharmacological and minimally invasive treatment of advanced heart failure (HF). The actual degree of heart failure is determined with the New York Heart Association (NYHA) functional scale and referred on the Interagency Registry for Mechanically Assisted Circulatory Support (INTERMACS) profiles, which provide important prognostic information for HF patients with MCS. The HF is a complex set of clinical symptoms that are characterized by an insufficient blood supply in accordance with the body's metabolic needs. The number of patients suffering from heart insufficiency increases every year. Meanwhile, the number of successful heart transplants has remained stable. The number of organ donors, including the heart, is limited, while the MCS systems often give patients time to wait for transplantation. In the case of long-term MCS the Continuous Flow Ventricular Assist Devices (CFVAD) (FIG. 1) are the most commonly used.

The implantation of the blood pump stops the expanding ischemia zone, provides the relief of the weakened heart and increases coronary perfusion, but - above all - it improves the cardiovascular hemodynamic. The fast development of technology brought about a variety of MCS solutions on the market, including LVAD (Left Ventricular Assist Device) for left ventricular support, RVAD (Right Ventricular Device) for right ventricular support and BIVAD (Biventricular Assist Device) for the assistance of both ventricles.

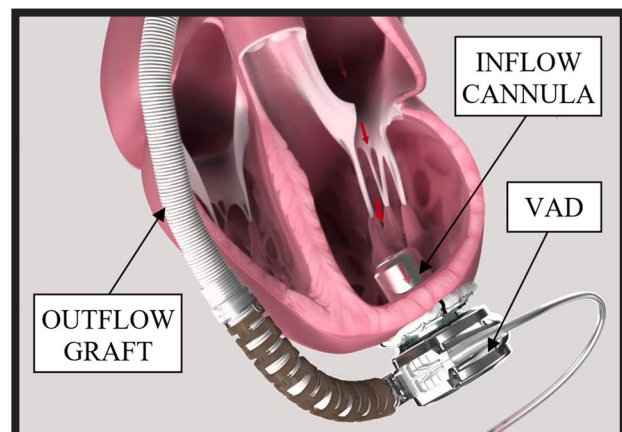


FIG. 1. The position of the implanted VAD on the example of MEDTRONIC HEARTWARE® pump [8].

VADs were developed to improve the failing heart function without replacing the biological organ. The methods of MCS can be described according to the diagnosis and prognosis of assistance goal and duration as: Bridge To Decision (BTD), Bridge To Recovery (BTR), Bridge To Transplant (BTT) and the Destination Therapy (DT) [9].

After many years of work, extracorporeal pulsatile VADs were replaced by new generations of implantable continuous flow (CF) devices in long term assistance [10]. So far, the clinical experience has shown that present-day pump constructions still need to be improved to minimize the risk of complications during heart assistance. In comparison to older constructions, there is a huge improvement thanks to the most modern biocompatible materials and surface engineering, along with the VAD miniaturization, limitation of its complexity and removal of mechanical bearings systems. Despite many new solutions, patients still experience high morbidity, many side effects and mortality. Actual VAD constructions consist of many components that may fail. As the pump is fully implantable, the procedure is difficult, invasive and requires the use of systemic anticoagulation. Moreover, the patients themselves become more complex and undergo VAD implantation in an increasingly critical form, causing many postoperative and direct support complications. One of the most important complications is embolization of the pump which may be caused by thrombus formation resulting from the thrombocyte activation. The thrombus may form in any part of the pump on the surfaces which stay in direct contact with blood. Bleeding and thrombotic complications are strongly related with haemostasis affected by antithrombotic and/or antiplatelet treatment. So the optimal balance is sometimes a challenge. However, there is still room to improve the pump construction to minimize blood clotting. One way is to change the design of the inflow cannula, its tissue attachment, as well as the length, location, and orientation of its introduction into the heart left ventricle. There is still no perfect solution and each device utilizes its own cannula design.

## Materials and Methods

The main goal of the project is to develop coating for the external surface of the inflow cannula of the Polish CF-VAD RELIGA HEART ROT [11] (FIG. 2) to provide the controlled myocardial tissue ingrowth around the cannula external wall. The clinical records exhibit the high importance of this phenomenon. The smooth external surface of the inflow cannula in the CF pump may cause the growth of tissue upwards the cannula inflow orifice, which may result in adverse flow turbulences or suction events disrupting the proper work of the inflow cannula.

The pump inflow obstruction is one of complications which are directly connected to the external surface of the inflow cannula design. It is caused by the tissue ingrowth into the flow passage, resulting in the pump flow collapse and possible pump thrombosis. According to the literature, the surface of the confluent cells monolayer may prevent thrombogenicity and develop an ideal blood-contacting surface eliminating the platelet deposition. The key role is played here by the surface topography including the presence of grooves, ridges, hills or pores. The textured topography represents the three-dimensional morphology, therefore it cannot be sufficiently characterized by only the linear profile. It requires additional measurement methods, such as Scanning Electron Microscopy (SEM), Energy-dispersive X-ray spectroscopy (EDS), atomic force microscope (AFM) and optical profilometer.

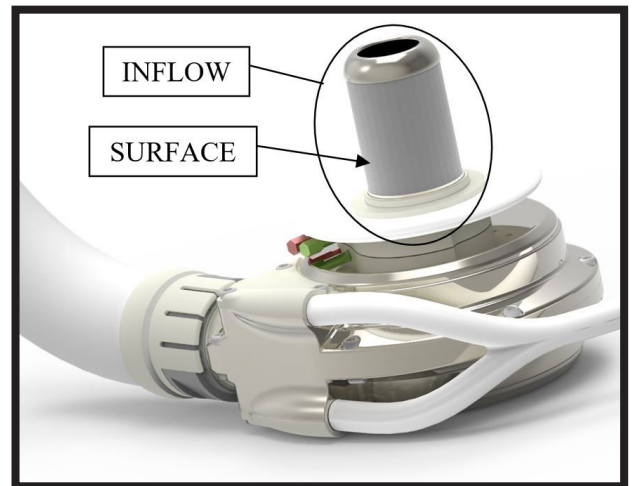


**FIG. 2.** The 3D visualization of the RELIGA HEART ROT pump under development in the Foundation of Cardiac Surgery Development in Zabrze, Poland.

The majors on the market are currently MEDTRONIC® with HEARTWARE (HW) ventricular assist system (VAS) and ABBOTT® with HEARTMATE III (HM3) VAS. However, there are many other VAD devised used in the clinical practice or during preclinical trials. The titanium alloy is the most common material used for the inflow cannulas and as the pump of most systems. Below there are presented VADs with modified inflow cannulas – FIG. 3. Every VAD is characterized by the different design of the inflow cannula, although many similarities can also be observed.

It is also worth noting that the surface modification was performed only on the external side of the inflow cannula in the case of HeartWare, Evaheart and Jarvik. This surface mainly contacts the heart muscle tissue and a small volume of flowing blood. However, the HeartMate II and HeartMate III have both external and internal surfaces subjected to spherical modifications. Similarly to other constructions, the external surface of the inflow cannula interfaces with the heart muscle tissue, whereas the internal porous surface is subjected to dynamic blood flows, which requires shear stress limitation and simultaneous stimulation of the protein film formation.

The clinical experience has confirmed positive effects of applying surface coating on the inflow cannula. Samer S. Najjar et al. performed the analysis of 382 patients who underwent the HVAD implantation to evaluate the statistics on the pump thrombus and treatment outcomes. One of the analyzed issues was the application of the inflow cannula coating. The original design of HVAD included highly polished titanium alloy on internal and external surfaces of the inflow cannula. However, the examinations of the explanted heart showed the tissue ingrowth encircling the external surface, which may be a source of emboli – FIG. 4a. Therefore, the modification of the inflow cannula was performed. To create a matrix enhancing the tissue ingrowth, the external surface was covered with the titanium microspheres via sintering. Thus, the tissue surrounding the well-polished inflow cannula did not adhere to the pump surface and may continue to grow upwards the orifice of the inflow cannula. The microspherical coating on the HVAD inflow cannula allowed the controlled growth of tissue in the coated area and limited the tissue overgrowth upwards the cannula. Yet, the paper did not show the direct impact of surface modifications on the thrombus events limitation, as the longer observation period was required to conclude [17].

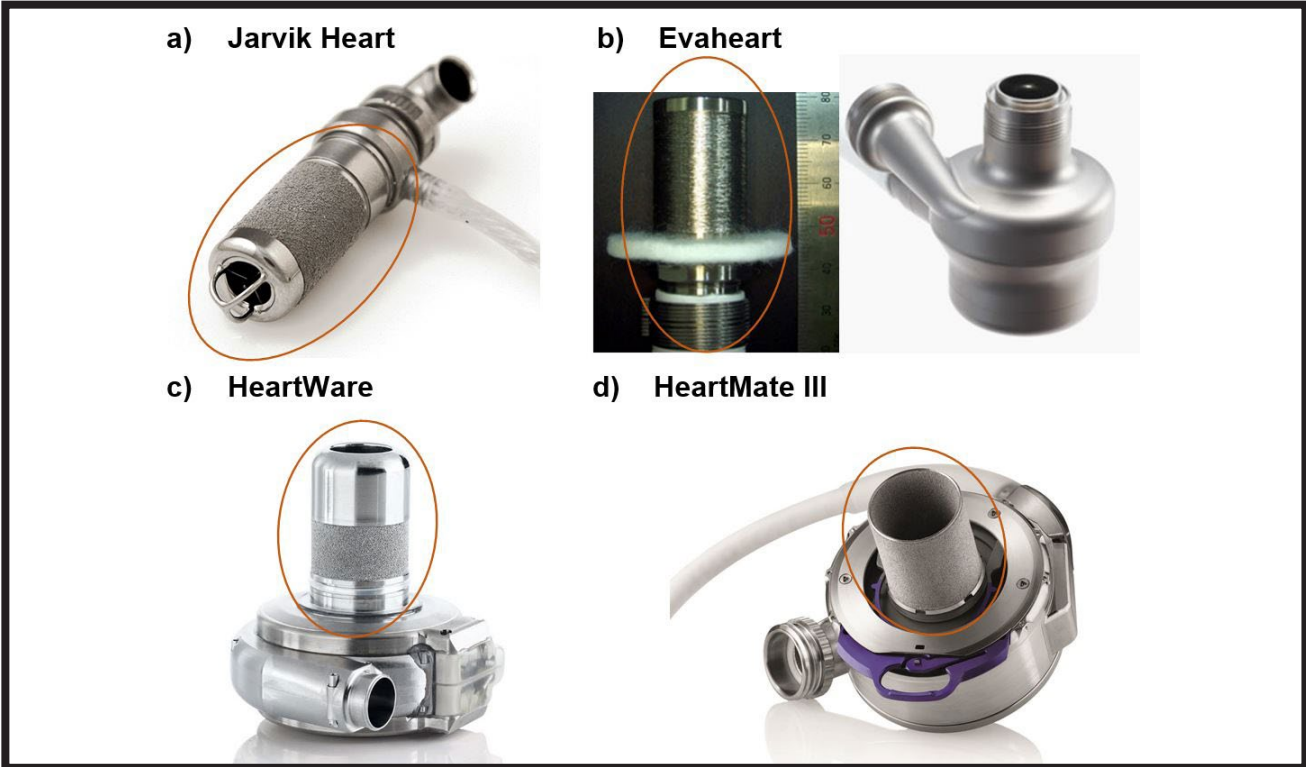


FIG. 3. Four VAD construction with presented inflow cannulas: a) Jarvik Heart [12], b) Evaheart [13,14], c) HeartWare [15], d) HeartMate III [16].

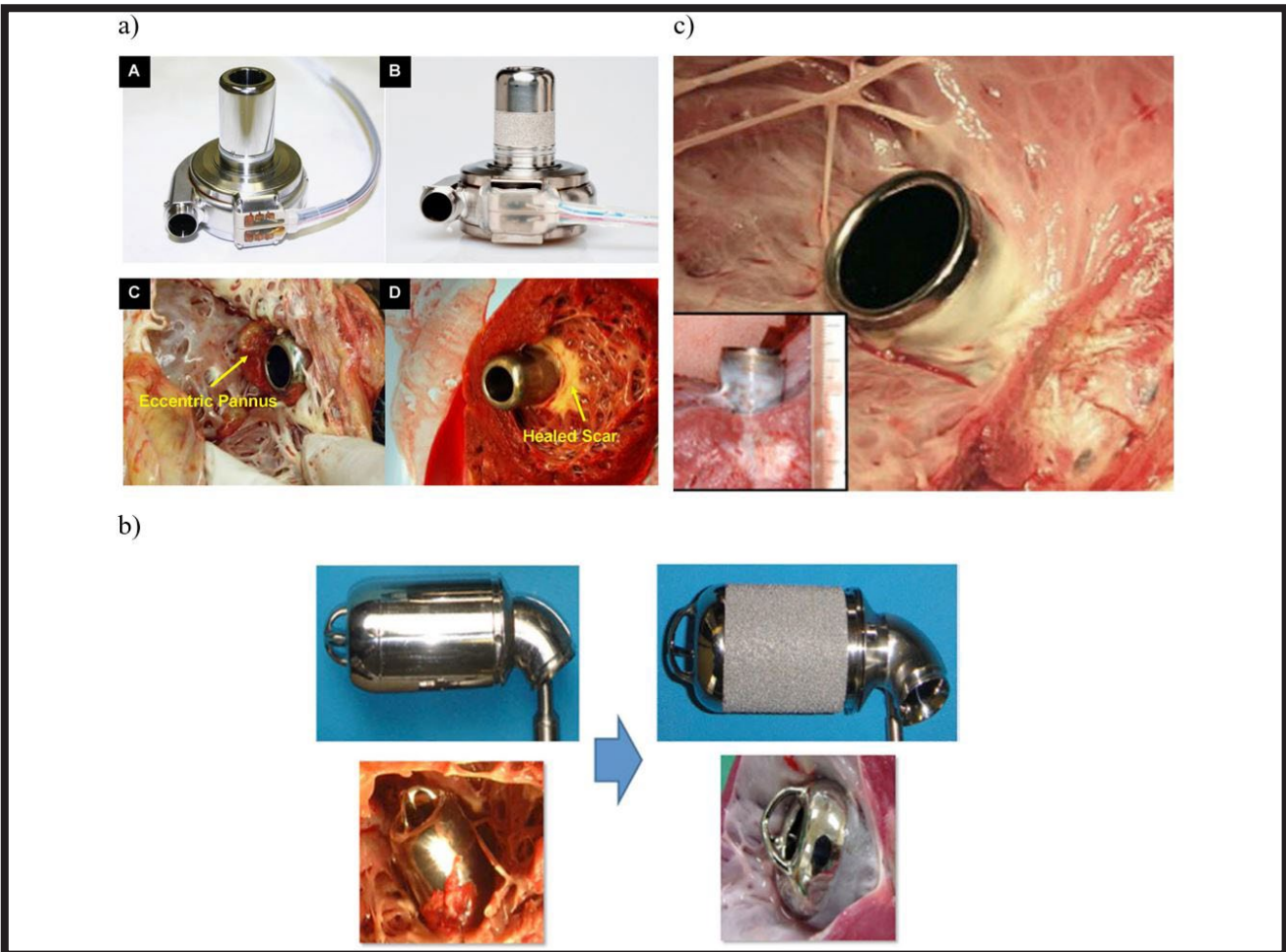


FIG. 4. Tissue ingrowth after surface modifications on the inflow cannulas of: a) Heartware [17], b) Jarvik 2000 [18], c) Evaheart [13].



Craig H. Selzman et al. presented a paper on Jarvik 2000 improvements to eliminate adverse events related to the pump thrombus and embolic events. One of the solutions was a modification of the inflow cannula design and the use of microsphere coating. The angle between the pump and the surrounding ventricular endocardium may result in the blood stasis and formation of thrombus. The external surface of the inflow cannula was modified within titanium microspheres to improve tissue adherence, provide better healing and reduce the risk of wedge thrombus formation – FIG. 4b [18].

Yukiko Yamada et al. hypothesized that the titanium mesh scaffold commonly used for cell culture could promote the growth of neointima, which would suppress the thrombus formation. The titanium wire of a diameter 85  $\mu\text{m}$  was wrapped around the inflow cannula creating a textured external surface characterized by the volumetric porosity of 40-70%. The mesh was then treated with high temperature to bond titanium fibers to the substrate. The wire structure was developed on the external surface of the inflow cannula on the section of <20 mm in length. To prevent the tissue overgrowth, an area of unmodified surface was left between the mesh tip and the cannula. The animal trials were performed on four healthy calves weighing 81-98 kg that were sacrificed humanely after 2 months. The analysis after the ex-plantation revealed white neointimal tissue on the titanium mesh structure without any wedge thrombus formation around the tip of the inflow cannula – FIG. 4c. A single layer of endothelial-like cells and mature connective tissue was detected during histological studies. The surface coating, which induces the ingrowth of autologous neointima, may result in limitation of thromboembolic events related to wedge thrombus, but also may allow the clinical introduction of less stringent anticoagulation procedures [13].

The presented studies confirm the necessity of surface modifications to enhance tissue ingrowth to the inflow cannula, which will minimize the risk of thrombus formation and pump embolization. This paper focuses on the physicochemical analysis of the porous surfaces developed in HeartMate III and HeartWare. The study includes the use of MarSurf XR for roughness measurements – FIG. 5, the Scanning Electron Microscopy (SEM) for morphology analysis with the dimensions measurements, the Energy-dispersive X-ray spectroscopy (EDS) for the surface composition study and the contact angle test using goniometric method.

The roughness measurements were performed in the axial direction of the inflow cannula. In order to preserve statistics, 5 measurements were taken for each sample. The roughness results are presented in TABLE 1, however parameters are very similar for both HM3 and HW. Additionally, the microcontour function was used to assess the step between the polished and porous surface of the HeartWare inflow cannula, which equals  $\sim 200 \mu\text{m}$ . In the case of HeartMate III the modified surface covers the whole inflow cannula – no step is observed.

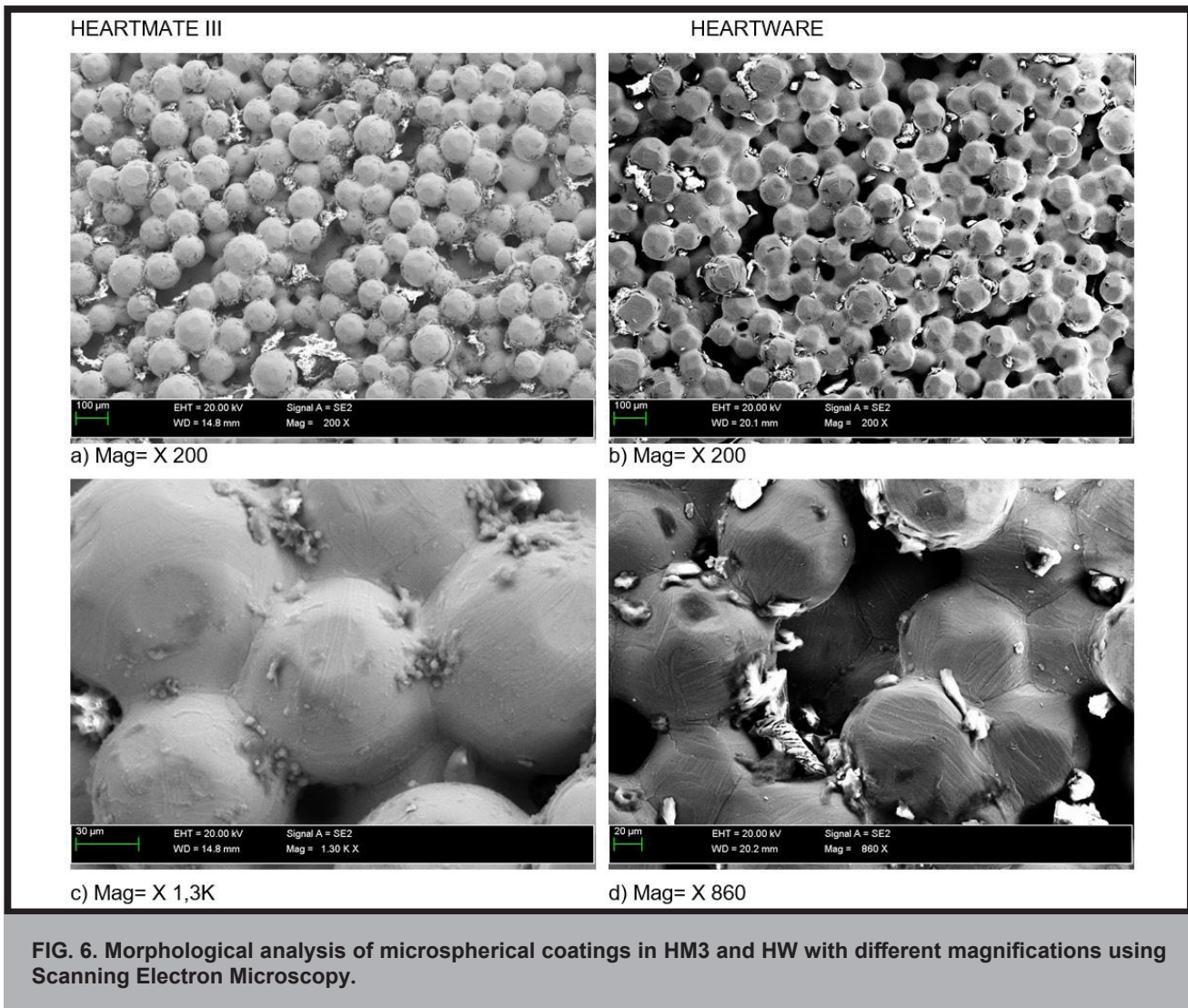
The SEM analysis revealed the microspherical morphology of the surface in the inflow cannulas of both the HeartMate III and HeartWare VADs – FIG. 6ab. The surfaces were probably subjected to the sintering process and most of the microspheres partially melted to each other. In the case of HM3 the surface consists of microspheres of 130  $\mu\text{m}$  mean diameter and includes 3 spherical layers. The actual thickness of coating is  $\sim 300 \mu\text{m}$ . The surface morphology is characterized by high porosity with inhomogeneous pore sizes in the range of 1-200  $\mu\text{m}$ . Such porosity allows migration and penetration of cells deep into the coating, enhancing tissue adhesion to the substrate. In the case of HW the surface is covered with microspheres of 115  $\mu\text{m}$  mean diameter. The thickness of the coating is  $\sim 200 \mu\text{m}$  and consists mainly of 2 spherical layers. Similarly to HM3, the surface of HW is characterized by high porosity and loose packing of the spheres on the cannula surface with inhomogeneous pore sizes in the range of 1-250  $\mu\text{m}$ . The pore sizes were estimated by means of microscopic observations using SEM. It is necessary to use a more precise test method to obtain more reliable data regarding the degree of porosity and average pore sizes. For both devices, the magnification in the 860-1,3k range revealed the mechanical deformations of spheres, a result of thermal stresses during the sintering process – FIG. 6cd.

TABLE 1. Roughness measurements obtained for HM3 and HW.

Roughness parameter	HeartMate III		HeartWare	
	Arithmetic mean value	Standard deviation	Arithmetic mean value	Standard deviation
Ra [ $\mu\text{m}$ ]	14.57	2.07	12.30	1.98
Rq [ $\mu\text{m}$ ]	17.73	2.74	15.38	2.50
Rz [ $\mu\text{m}$ ]	72.77	12.05	66.21	10.90
Rt [ $\mu\text{m}$ ]	90.23	18.83	89.98	14.62



FIG. 5. The MarSurf XR measuring unit and exemplary measurement.



The EDS analysis performed on the microspheres have shown the composition of Ti, Al, V. The HM3 surface consists of Ti = 92.68%, Al = 4.73%, V = 2.59%, however the HW surface includes Ti = 91.48%, Al = 3.66%, V = 4.86%. For both devices, the surface was characterized as the titanium alloy Ti6Al4V, which confirmed the information disclosed by the manufacturer. The Ti6Al4V alloy is the most widely used material to manufacture implants because of its high biocompatibility and corrosion resistance. However, according to literature, vanadium (V) may cause potential cytotoxicity and adverse tissue reactions. Nowadays, the Ti6Al7Nb alloy is becoming more and more often used for long-term medical implants.

The investigation of the contact angle was carried out on the samples at 20 °C with the Möller-Wedel Optical apparatus, using the goniometric method – FIG. 7. The distilled water was applied on the sample surface with a volume of the 1.5 µl measuring drop.

In order to preserve statistics, 5 measurements were taken for each sample. The samples were cleaned and dried from the residual water, using compressed air before each measurement. The measurements were performed for the spherical surface of HM3 and HW. In the first case the surface was characterized by the contact angle of  $\phi = 72.4^\circ$ . In the case of HW the contact angle was equal to  $\phi = 69.3^\circ$ . The obtained results for both devices allowed determining the wettability characteristics of modified surfaces which proved to be highly hydrophilic. The good wettability has a positive effect on the cell migration in the area of surface modification, which results in good tissue ingrowth.

## Results and Discussions

Currently surface modifications of medical implants provide enormous opportunities to customize and functionalize implant-tissue connections. The phenomenon of bone tissue growth has already been successfully investigated in the clinical practice. Unfortunately, the issues of cardiac surgical implants have not found such interest so far, despite the widespread use of mechanical circulatory support systems. There is still a lack of detailed data on advanced assessment of the phenomena occurring in the heart muscle at the tissue-inflow cannula interface. There are no data in the literature which determines the morphological parameters of the surface coating that would provide a permanent and stable connection of the cardiac support device with myocardial tissue. The clinical experience has shown the positive influence of surface modifications on the inflow cannula. On the basis of actual literature, the microspherical coating on the inflow cannula of HVAD allowed the controlled growth of tissue and limited the tissue overgrowth upwards the cannula. On the other hand, the surface modification which stimulates the ingrowth of autologous neointima may limit thromboembolic events related to wedge thrombus, possibly allowing the clinical introduction of less stringent anticoagulation procedures. The presented studies confirm the necessity of surface modification to enhance tissue ingrowth to the inflow cannula, which will minimize the risk of the thrombus formation and pump embolization.

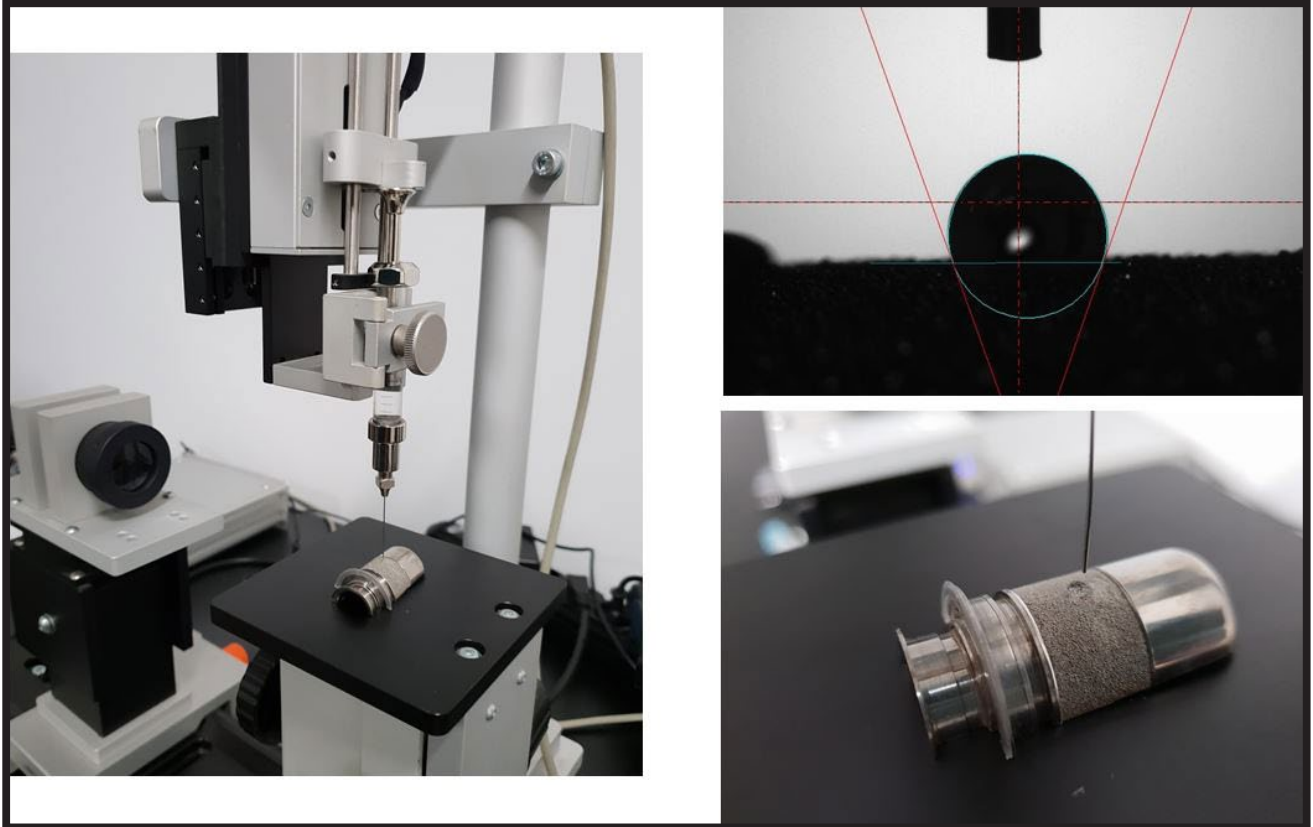


FIG. 7. Wettability measurements performed for HM3 and HW with exemplary result.

The physicochemical analysis of the porous surfaces on the inflow cannulas of the two VADs was performed. The SEM analysis revealed the microspherical morphology of the surface in both cases. The mean diameter of spheres observed in HM3 is 130  $\mu\text{m}$ , however in HW it is 115  $\mu\text{m}$ . Both surfaces are characterized by high porosity and loose packing of spheres on the cannula surface. Pore sizes are inhomogeneous and vary in the range of 1-200  $\mu\text{m}$  for HM3, and 1-250  $\mu\text{m}$  for HW, respectively. The HM3 coating consists of 3 spherical layers, while in HW there are just 2 layers. Consequently, the thickness is  $\sim 300$   $\mu\text{m}$  for HM3 and  $\sim 200$   $\mu\text{m}$  for HW. In both cases, the surface was characterized as the titanium alloy Ti6Al4V. The external surface of the inflow cannula for both VADs was characterized by similar roughness of Ra (12-15  $\mu\text{m}$ ) and Rz (66-73  $\mu\text{m}$ ) parameters. The contact angle measurement for both devices allowed determining the wettability characteristics of modified surfaces which proved to be highly hydrophilic. Further research is needed to collect data on the cellular profile of tissues in the contact area with the biomaterial.

## Conclusions

So far, the clinical research has shown that VAD pumps still need to be improved in order to minimize the risk of complications during heart assistance. In comparison to older systems, there is a huge improvement through the application of modern biocompatible materials and surface engineering, accompanied by the VAD minimalization, the complex limitation of its complexity and removal of mechanical bearings systems. Despite many new solutions, patients still experience many side effects, including high morbidity and even death. One of the complications directly connected to the inflow cannula design is the inflow obstruction, caused by the ingrowth of tissue into the flow passage and pump thrombosis.

The solution may be improving the design of the inflow cannula, its attachment, as well as the length, location, and orientation of its introduction or development of the bioactive surface. There is still no perfect solution and each device has its own cannula design with different external surfaces promoting cell adhesion. The clinical experience confirms that thanks to the developed surfaces, it is possible to control the tissue ingrowth on the external surfaces of the inflow cannula at the tissue-implant interface. However, it is still necessary to perform more trials to provide a better understanding of the phenomena occurring at the implant-tissue interface.

## Acknowledgments

*Project supported by NCBiR within the project RH-ROT/266798/STRATEGMED-II.*

*Project co-financed by National Science Centre, Poland within the project PRELUDIUM 16 2018/31/N/ST8/01085.*

## ORCID iDs

P. Kurtyka: <https://orcid.org/0000-0001-8692-0737>  
 R. Kustosz: <https://orcid.org/0000-0002-9268-7529>  
 M. Kaczmarek: <https://orcid.org/0000-0002-0049-1554>  
 M. Gonsior: <https://orcid.org/0000-0002-1970-1937>  
 K. Tokarska: <https://orcid.org/0000-0001-8796-5478>

## References

- [1] L. Ramaglia, G. Capece, G. Di Spigna, M. P. Bruno, N. Buonocore, L. Postiglione: Effects of titanium surface topography on morphology and in vitro activity of human gingival fibroblasts. *Minerva Stomatol.* 62(7-8) (2013) 267-80.
- [2] Z. Zhang, H. Kurita, H. Kobayashi, K. Kurashina: Osteoinduction with HA/TCP Ceramics of Different Composition and Porous Structure in Rabbits. *Oral Sci. Int.*, 2(2) (2005) 85-95.
- [3] C. Wang et al.: Bone growth is enhanced by novel bioceramic coatings on Ti alloy implants. *J. Biomed. Mater. Res. Part A*, 90A(2) (2009) 419-428.
- [4] M. Rouahi, O. Gallet, E. Champion, J. Dentzer, P. Hardouin, K. Anselme: Influence of hydroxyapatite microstructure on human bone cell response. *J. Biomed. Mater. Res. Part A* 78A(2) (2006) 222-235.
- [5] J.D. Bobyne, R.M. Pilliar, H.U. Cameron, G.C. Weatherly: The optimum pore size for the fixation of porous-surfaced metal implants by the ingrowth of bone. *Clin. Orthop. Relat. Res.* 150 (1980) 263-270.
- [6] B. Levine: A New Era in Porous Metals: Applications in Orthopaedics. *Adv. Eng. Mater.* 10(9) (2008) 788-792.
- [7] J. Bieniek, Z. Swiecki: Porous and porous-compact ceramics in orthopedics. *Clin. Orthop. Relat. Res.* 272 (1991) 88-94.
- [8] "maxresdefault.jpg (1280×720)." [Online]. Available: <https://i.ytimg.com/vi/ucgU4u9e4Gk/maxresdefault.jpg>.
- [9] "Clinical Cardiology: Current Practice Guidelines - Demosthenes G. Katritsis, Bernard J. Gersh, A. John Camm [Online]. Available: <https://books.google.pl/books?id=OrISDQAAQBAJ&pg=PA404&lpg=PA404&dq=btd+btr+btt+dt&source=bl&ots=-whh12aSHi&sig=ACfU3U0FKq09Xu7Ko8ueziQHlJrrsCVnMA&hl=pl&sa=X&ved=2ahUKEwiPk7jL8NDIAhUEXosKHVOVBqUQ6AEwAnoECAkQAQ#v=onepage&q=btd+btr+btt+dt&f=false>.
- [10] J.K. Kirklin et al.: Seventh INTERMACS annual report: 15,000 patients and counting. *J. Hear. Lung Transplant.* 34(12) (2015) 1495-1504.
- [11] S. Stano, R. Kustos, A. Kapis, P. Kurtyka, J. Zalewski, M. Zarwańska: Influence of the laser welding process on changes in the magnetic induction of the Religa Heart ROT pump. *Weld. Technol. Rev.* 91(4) (2019) 39-47.
- [12] "Jarvik-15mm-LVAD.png (770×575)." [Online]. Available: <http://www.medgadget.com/wp-content/uploads/2016/10/Jarvik-15mm-LVAD.png>.
- [13] Y. Yamada, T. Nishinaka, T. Mizuno, Y. Taenaka, E. Tatsumi, K. Yamazaki: Neointima-inducing inflow cannula with titanium mesh for left ventricular assist device. *J. Artif. Organs* 14(4) (2011) 269-275.
- [14] "eveheart-01.jpg (460×280)." [Online]. Available: <http://www.evaheart.co.jp/images/evaheart/eveheart-01.jpg>.
- [15] "heartware-office.jpg (1000×769)." [Online]. Available: <https://media.glassdoor.com/l/116921/heartware-office.jpg>.
- [16] "ows\_153998639894175.jpg (2000×1503)." [Online]. Available: [http://stmedia.stimg.co/ows\\_153998639894175.jpg?fit=crop&crop=faces](http://stmedia.stimg.co/ows_153998639894175.jpg?fit=crop&crop=faces).
- [17] S.S. Najjar et al.: An analysis of pump thrombus events in patients in the HeartWare ADVANCE bridge to transplant and continued access protocol trial. *J. Hear. Lung Transplant.* 33(1) (2014) 23-34.
- [18] C.H. Selzman, A. Koliopoulou, J.P. Glotzbach, S.H. McKellar: Evolutionary improvements in the jarvik 2000 left ventricular assist device. *ASAIO J.* 64(6) (2018) 827-830.

# OSTEOBLASTS RESPONSE TO NOVEL CHITOSAN/AGAROSE/HYDROXYAPATITE BONE SCAFFOLD – STUDIES ON MC3T3-E1 AND HFOB 1.19 CELLULAR MODELS

PAULINA KAZIMIERCZAK<sup>ID</sup>, VLADYSLAV VIVCHARENKO<sup>ID</sup>, WIESŁAW TRUSZKIEWICZ<sup>ID</sup>, MICHAŁ WÓJCIK<sup>ID</sup>, AGATA PRZEKORA\*<sup>ID</sup>

DEPARTMENT OF BIOCHEMISTRY AND BIOTECHNOLOGY,  
MEDICAL UNIVERSITY OF LUBLIN,  
CHODZKI 1, 20-093 LUBLIN, POLAND  
\*E-MAIL: AGATA.PRZEKORA@UMLUB.PL

## Abstract

Since it is known that various cell lines may express different behaviours on the scaffolds surface, a comprehensive analysis using various cellular models is needed to evaluate the biomedical potential of developed biomaterials under *in vitro* conditions. Thus, the aim of this work was to fabricate bone scaffolds composed of a chitosan-agarose matrix reinforced with nanohydroxyapatite and compare the biological response of two cell lines, i.e. mouse calvarial preosteoblasts (MC3T3-E1 Subclone 4) and human foetal osteoblasts (hFOB 1.19). Within this study, the osteoblasts number on the scaffold surface and the osteogenic markers level produced by MC3T3-E1 and hFOB 1.19 cells were determined. Furthermore, changes in calcium and phosphorous ions concentrations in the culture media dedicated for MC3T3-E1 and hFOB 1.19 were estimated after the biomaterial incubation.

The obtained results proved that the fabricated biomaterial is characterized by biocompatibility and osteoconductivity since it favours osteoblasts attachment and growth. It also supports the production of osteogenic markers (collagen, bALP, osteocalcin) by MC3T3-E1 and hFOB 1.19 cells. Interestingly, the developed biomaterial exhibits different ion reactivity values in the two culture media dedicated for the mentioned cell lines. It was also revealed that mouse and human osteoblasts differ in the cellular response to the fabricated scaffold. Thus, the use of at least two various cellular models is recommended to carry out a reliable biological characterization of the novel biomaterial. These results demonstrate that the tested bone scaffold is a promising biomaterial for bone regeneration applications, however further biological and physicochemical experiments are essential to fully assess its biomedical potential.

**Keywords:** bone tissue engineering, biocompatibility, osteoconductivity, cell growth, osteogenic differentiation

[*Engineering of Biomaterials* 151 (2019) 24-29]

## Introduction

Bone grafting is a routinely applied treatment in regenerative medicine. Despite the high efficiency of bone tissue transplantations, this treatment is constrained by painful procedures of tissue harvesting, donor-site morbidity, potential infections, disease transmission and anatomical limitations. Thus, whenever the application of bone grafts is impossible, tissue-engineered constructs are used in regenerative medicine [1,2]. Typical bone scaffolds applied in bone tissue engineering (BTE) are characterized by a three-dimensional (3D) structure which imitates the microstructure of natural bone. BTE involves the use of biomaterials as cellular devices or as scaffolds combined with cells, growth factors and/or drugs [3].

It is worth emphasizing that tissue-engineered constructs should trigger the right host response without side effects, e.g. chronic inflammation or immune rejection [4]. In order to assess the medical potential of fabricated scaffolds under *in vitro* conditions, the biomaterials are subjected to a comprehensive analysis using various cellular models [5,6]. The cellular response to the bone scaffolds depends on many features of the biomaterials. First of all, the architecture of scaffolds is of critical importance. Bone scaffolds should be characterized by high porosity with interconnected pore structure to ensure space for cells penetration and new vascular network formation. Moreover, the biomaterial porous structure allows nutrients and waste products diffusion and ensures good oxygenation [1,7,8]. Another critical feature is the pores size within the solid structure of the scaffold. According to the available literature, the pore size of at least 100 µm is considered crucial for bone ingrowth [7]. Furthermore, scaffolds for BTE applications should have adequate mechanical properties to withstand loads at the implantation site [9]. The chemical characteristics of the scaffold surface, such as charge, functional groups and wettability, also affect cell behaviour. The polar and positively charged surface supports the cell attachment and spreading [10], whereas the hydrophilic surface favours the adsorption of cell adhesive proteins (e.g. laminin, vitronectin, fibronectin) [6,11]. Likewise, the rough bone scaffold surface facilitates the proteins adsorption [8,10], which is critical for cell attachment, spreading, and proliferation. It is worth noting that cells do not interact directly with the biomaterial surface but with the adsorbed proteins [6].

As it was mentioned above, the cellular response to tissue-engineered constructs may depend on many factors. Thus, novel scaffolds should be subjected to a complete biological and physicochemical analysis. In this study, we fabricated the highly porous scaffold composed of the chitosan-agarose matrix reinforced with the hydroxyapatite nanopowder. The scaffold composition was to mimic bone and accelerate bone regeneration. The polysaccharide matrix was designed to imitate flexible organic parts of bone, whereas the synthetic hydroxyapatite nanopowder was to mimic the natural bone mineral [6]. Moreover, in order to obtain a highly porous structure with interconnected pores, we produced the scaffold applying a gas-foaming agent and the freeze-drying method simultaneously. Both the scaffold composition and the applied production method are characterized by high novelty and claimed in the Polish patent application no P.426788. The novel scaffold was proved to have the total open porosity (approx. 70%) and the compressive strength values (1.4 MPa) comparable to cancellous bone. Moreover, the chitosan/agarose/hydroxyapatite material is non-toxic and it favours the cell attachment and spreading [12].

Since it is known that various cell lines may exhibit different behaviours on the biomaterial surface, the primary goal of this work was to evaluate and compare the biological response of the mouse calvarial preosteoblast cell line (MC3T3-E1 Subclone 4) and the normal human foetal osteoblast cell line (hFOB 1.19) to the fabricated scaffold. Within this study, we evaluated the osteoblasts number after the 3-day culture on the biomaterial surface and the level of osteogenic markers produced by the mouse MC3T3-E1 cells and the human hFOB 1.19 ones. Additionally, changes in calcium ( $\text{Ca}^{2+}$ ) and phosphorous ( $\text{HPO}_4^{2-}$ ) concentrations in the culture media (dedicated for MC3T3-E1 and hFOB 1.19 cells) after incubating the scaffold were assessed. Thus we determined the ion reactivity of the material which also may influence the cellular response.

## Materials and Methods

### Materials

Chitosan, agarose, hydroxyapatite nanopowder (nanoHA) and sodium bicarbonate ( $\text{NaHCO}_3$ ) were purchased from Sigma-Aldrich Chemicals. Acetic acid ( $\text{CH}_3\text{COOH}$ ) and sodium hydroxide solution ( $\text{NaOH}$ ) were obtained from Avantor Performance Materials. Cell experiments were performed using osteoblast cell lines: the mouse calvarial preosteoblast cell line (MC3T3-E1 Subclone 4) and the normal human foetal osteoblast cell line (hFOB 1.19), which were purchased from American Type Culture Collection (ATCC). The Alpha-MEM medium was obtained from Gibco, USA. The DMEM/Ham F12 medium without phenol red, the 0.25% trypsin-EDTA solution, the penicillin-streptomycin solution, the G418 disulfate salt solution, ascorbic acid,  $\beta$ -glycerophosphate, dexamethasone, paraformaldehyde, Triton X-100, bovine serum albumin (BSA) and DAPI were obtained from Sigma-Aldrich Chemicals. Lactate Dehydrogenase Activity Assay Kit (LDH) was also obtained from Sigma-Aldrich Chemicals. Foetal bovine serum (FBS) was purchased from Pan-Biotech GmbH.  $\text{Ca}^{2+}$  and  $\text{HPO}_4^{2-}$  ions concentrations in media were estimated using Calcium CPC and Phosphorous Assay Kits, which were acquired from Biomaxima. AlexaFluor635-conjugated phallotoxin was obtained from Invitrogen. Bone alkaline phosphatase (bALP) activity in cell lysates was measured using the mouse-specific ELISA assay (Mouse Bone Alkaline Phosphatase ELISA Kit) and the human-specific ELISA assay (Human Bone Alkaline Phosphatase ELISA Kit) obtained from FineTest. Type I collagen (Col I) and osteocalcin (OC) levels in cell lysates were measured using the mouse-specific ELISA assays (Mouse Collagen alpha-1(I) chain ELISA Kit, Mouse Osteocalcin ELISA Kit) and the human-specific ELISA assays (Human Collagen alpha-1(I) chain ELISA Kit, Human Osteocalcin ELISA Kit) supplied by EIAab.

### Scaffold production

The scaffold was synthesized via the simultaneous application of the gas-foaming agent and the freeze-drying method. Briefly, 2%w/v chitosan (75-85% deacetylation degree, viscosity  $\leq 300$  cP, 50-190 kDa molecular weight) and 5%w/v agarose (low EEO, gel point  $36 \pm 1.5^\circ\text{C}$ ) were suspended in 2%v/v  $\text{CH}_3\text{COOH}$ . Then, the obtained suspension was mixed with 40%w/v nanoHA and  $\text{NaHCO}_3$  (a foaming agent). The resultant paste was put into a cylinder-shaped form and subjected to heating in a water bath at  $95^\circ\text{C}$ . Then, the sample was cooled, frozen in a liquid vapour phase and lyophilized (LYO GT2-Basic). The final scaffold was neutralized in 1%w/v  $\text{NaOH}$  solution, washed with deionised water, and left to dry at room temperature. The scaffold was sterilized by ethylene oxide. The microstructure of the produced scaffold was visualized using a stereoscopic microscope (Olympus SZ61TR) (FIG. 1).

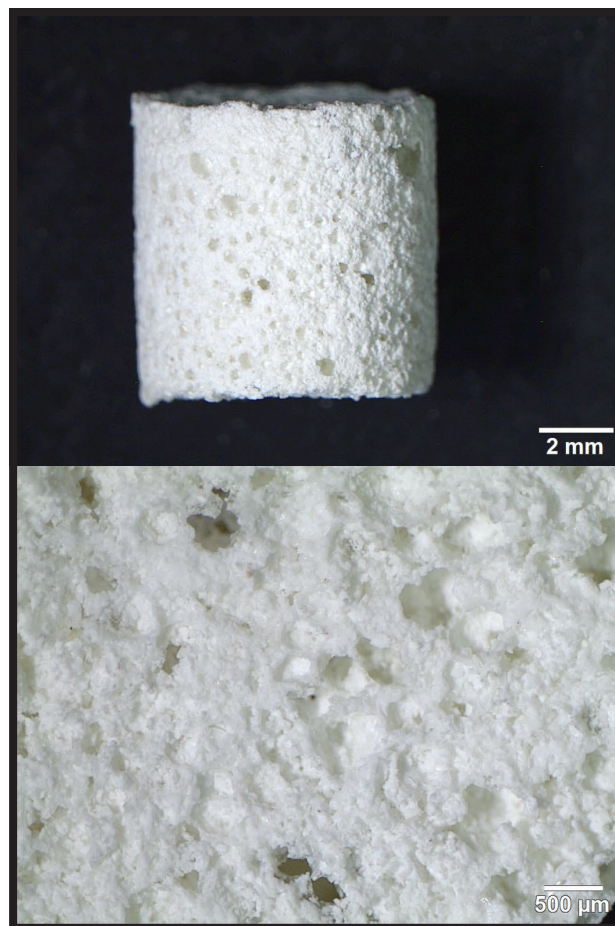


**FIG. 1. Microstructure of the fabricated scaffold visualized by a stereoscopic microscope.**

### Ion concentrations assessment

The changes in ion concentrations were estimated in the culture media (dedicated for MC3T3-E1 and hFOB 1.19 cells) after the incubation with the scaffold. The biomaterial discs were immersed in the alpha-MEM and DMEM/Ham F12 medium maintaining the proportion of 100 mg sample per 1 ml culture medium and incubated at  $37^\circ\text{C}$  for 24 h. Culture media without the scaffold were treated as the control media. After 24-h incubation with the scaffold, the culture media were collected by centrifugation and  $\text{Ca}^{2+}$  and  $\text{HPO}_4^{2-}$  concentrations were estimated spectrophotometrically using the Calcium CPC and Phosphorous Assay Kits following the manufacturer's protocol.

### Cell culture experiments

Prior to cell seeding onto the scaffold surface, the sample discs were placed in the wells of polystyrene plate and preincubated in the appropriate complete culture medium. The MC3T3-E1 cell line was maintained in the alpha-MEM medium supplemented with 10% FBS, 100 U/ml penicillin and 0.1 mg/ml streptomycin. The hFOB 1.19 cell line was maintained in the DMEM/Ham F12 medium without phenol red supplemented with 10% FBS, 300  $\mu\text{g}/\text{ml}$  G418, 100 U/ml penicillin and 0.1 mg/ml streptomycin. The MC3T3-E1 cells and the hFOB 1.19 cells were incubated in a humid atmosphere with 5%  $\text{CO}_2$  at  $37^\circ\text{C}$  and  $34^\circ\text{C}$ , respectively.

### Osteoblast number assessment

The assessment of osteoblast number on the scaffold surface was conducted after the 3-day culture. The MC3T3-E1 and hFOB 1.19 cells were seeded directly on the scaffold discs (4 mm in diameter and 2 mm thick), placed in a 96-wells plate in 100  $\mu$ l of the medium at the concentration of  $5 \times 10^4$  cells/ml. On the 3rd day, the cells grown on the surface of the scaffold were lysed, as described previously [13]. Then, the total cell number in lysates was estimated using LDH Activity Assay following the manufacturer's protocol. The exact number of cells was estimated using a calibration curve made for the known cell number of MC3T3-E1 cells and hFOB 1.19 cells.

Additionally, osteoblasts on the scaffold surface were visualized by fluorescent staining of cytoskeleton and nuclei. After the 3-day culture, the cells were fixed with 3.7%v/v paraformaldehyde, permeabilized with 0.2%v/v Triton X-100 and blocked with 1%w/v BSA. The cytoskeleton filaments and nuclei were stained with AlexaFluor635-conjugated phallotoxin and DAPI, respectively. The stained cells were visualized by confocal laser scanning microscope (CLSM).

### Evaluating the level of osteogenic markers

The osteogenic differentiation of the cells on the scaffold surface was carried out for 16 days. The MC3T3-E1 cells and the hFOB 1.19 cells were seeded directly on the scaffold discs (7 mm in diameter and 2 mm thick), placed in a 48-wells plate in 500  $\mu$ l of the appropriate complete culture medium at the concentration of  $4 \times 10^5$  cells/ml and incubated for 24 h at 37°C and 34°C, respectively. Then, the culture medium was discarded and replaced with the osteogenic medium made of the appropriate complete culture medium supplemented with 50  $\mu$ g/ml ascorbic acid, 0.01  $\mu$ M  $\beta$ -glycerophosphate, and 0.01  $\mu$ M dexamethasone. Every third day, half of the osteogenic medium was changed with a fresh portion. On the 8th and 16th day of the experiment, the cells were lysed, as described previously [13], and the level of osteogenic markers in cell lysates was estimated using appropriate ELISA assays for mouse and human species. The bALP activity and Col I concentration were estimated on the 8th day of the experiment, whereas the bALP activity and OC concentration were estimated on the 16th day of the experiment.

### Statistical analysis

All the experiments were conducted in triplicate ( $n = 3$ ) and the obtained results were showed as mean values  $\pm$  standard deviation (SD). The data were statistically analyzed using an unpaired t-test (GraphPad Prism 8.0.0 Software). Statistically significant differences were considered at  $p < 0.05$ .

## Results and Discussions

### Ion concentrations assessment

The surface of calcium phosphate-based biomaterials may interact with the ions which are present in the culture environment, causing fluctuation in ion concentrations which, in turn, may influence cellular response [14,15]. Thus, in this study, the evaluation of ion concentrations in the culture media after the scaffold incubation was performed. In this experiment, the media dedicated particularly for maintaining the MC3T3-E1 and the hFOB 1.19 cell were used. As shown in FIG. 2a, the biomaterial incubation in the culture medium dedicated for the MC3T3-E1 cell line resulted in the significant uptake of  $\text{Ca}^{2+}$  ions from the surrounding microenvironment. Interestingly, the divergent results were obtained for the scaffold incubated in the culture medium dedicated for the hFOB 1.19 cell line (FIG. 2b) where the significant release of  $\text{Ca}^{2+}$  ions was observed. As for the  $\text{HPO}_4^{2-}$  concentration in the culture media, it was revealed that the scaffold caused the significant uptake of these ions, regardless of the applied culture medium. The observed fluctuations in ion concentrations in the liquid environment are typical for calcium phosphate-based biomaterials. The uptake of  $\text{Ca}^{2+}$  and  $\text{HPO}_4^{2-}$  ions from the culture medium probably resulted from the electrostatic interaction between the charged biomaterial surface and ions in the culture microenvironment [16]. Moreover, this phenomenon may be also associated with the bone-like apatite formation on the scaffold surface [16,17]. The  $\text{Ca}^{2+}$  ions release was possibly caused by the hydroxyapatite dissolution or the ionic substitution of  $\text{Ca}^{2+}$  ions present in hydroxyapatite by other ions occurring in the culture medium [18].

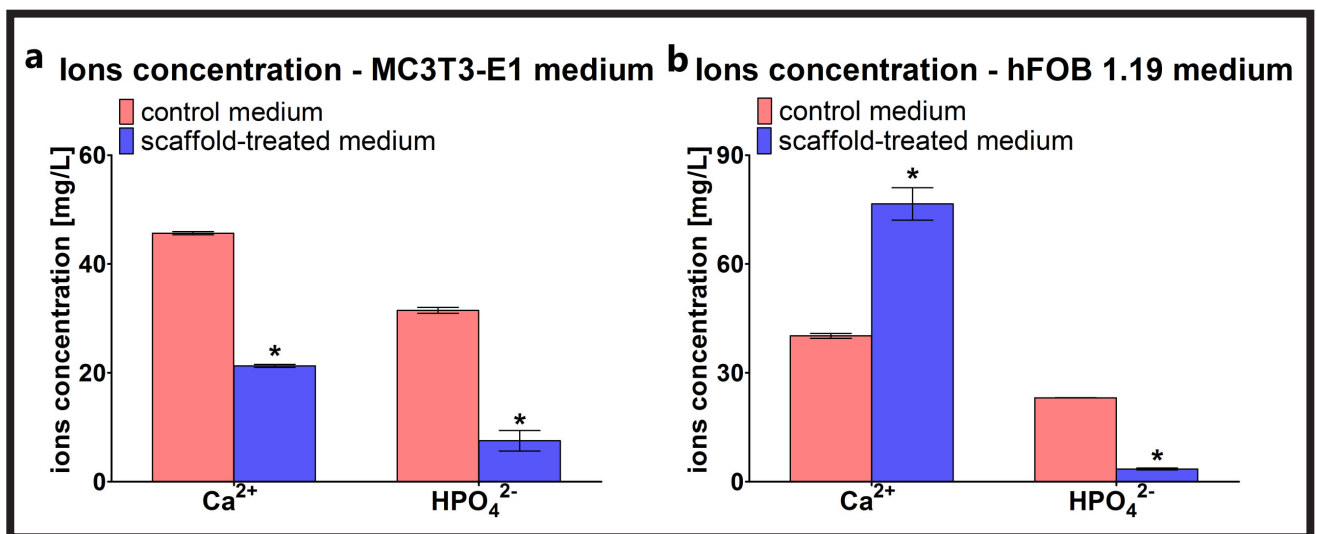


FIG. 2. Changes in  $\text{Ca}^{2+}$  and  $\text{HPO}_4^{2-}$  ions concentration [mg/L] in culture medium dedicated for (a) MC3T3-E1 and (b) hFOB 1.19 cells after incubation with the scaffold (scaffold-treated medium); \*statistically significant results compared to appropriate control medium ( $p < 0.05$ ,  $n = 4$ , unpaired t-test).

### Osteoblast number assessment

To compare cell behaviour of the two different osteoblast cell lines on the scaffold surface, the mouse (MC3T3-E1) and human (hFOB 1.19) osteoblasts were seeded directly on the scaffold and cultured for 3 days, then the cell numbers were evaluated by the LDH total test. FIG. 3 shows that after the 3-day culture, the number of the MC3T3-E1 cells was  $8.99 \pm 1.04 \times 10^3$ , whereas the number of the hFOB 1.19 cells equalled  $7.14 \pm 1.65 \times 10^3$ . Thus, the MC3T3-E1 cells were slightly more numerous on the material surface as compared to the hFOB 1.19 osteoblasts. However, the observed differences were not statistically significant. It should be noted that the cell growth on the scaffold surface may be affected by fluctuations in ion concentrations occurring in the surrounding culture medium. It is well known that extracellular  $\text{Ca}^{2+}$  ions support osteoblast adhesion, proliferation and extracellular matrix (ECM) formation [8]. However, too high  $\text{Ca}^{2+}$  concentrations in the culture microenvironment may lead to hyperosmotic stress causing cell shrinkage and intracellular dehydration, followed by cell death [19]. It was observed that the scaffold caused the increase in  $\text{Ca}^{2+}$  concentration in the culture medium dedicated for human osteoblasts. Thus, a slightly lower number of the hFOB 1.19 cells on the scaffold surface as compared to the mouse osteoblasts could result from local too high concentration of  $\text{Ca}^{2+}$  ions.

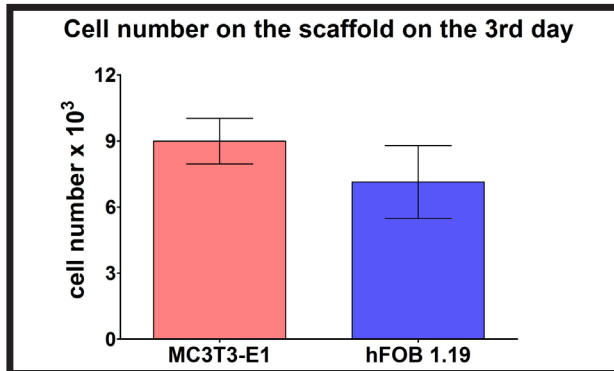


FIG. 3. Comparison of osteoblast number on the surface of the scaffold (n = 4, unpaired t-test).

The CLSM images showed that both the MC3T3-E1 cells and the hFOB 1.19 cells cultured on the scaffold surface were well spread and had flattened morphology (FIG. 4), proving that the surface of the fabricated scaffold supported the cell attachment and growth. Thus, the developed bio-material possesses osteoconductive properties which are defined as the ability of the scaffold to favour cell adhesion, growth, and differentiation [6].

### Evaluation of osteogenic markers level

The osteogenic differentiation of cells is a 3-step process involving: 1) intensive cell proliferation, 2) ECM synthesis, 3) ECM mineralization. During each phase of the osteogenic differentiation, cells produce specific osteogenic markers. During the proliferation stage, cells exhibit rapid proliferation and produce mainly a great amount of Col I and fibronectin. In the ECM synthesis stage, cells do not divide anymore and begin the intensive synthesis of the bone ECM proteins. Additionally, during this stage cells exhibit the highest bALP activity. In the third stage, cells reveal high mineralization activity. This phase is also characterized by high production of OC and osteopontin which are responsible for binding calcium ions and thus ECM mineralization. Importantly, during the ECM mineralization stage, the bALP activity is at a moderate level [6,20].

The evaluation of osteogenic cells differentiation on the surface of the engineered bone scaffold is crucial in terms of medical application. In this study, we tested *in vitro* two cellular models (MC3T3-E1 Subclone 4 and hFOB 1.19) which are commonly used in preclinical testing of biomaterials and are considered proper models for studying osteoblast behaviour and osteogenic differentiation [6]. The MC3T3-E1 cell line is known for cell proliferation and mineralization potential similar to human primary osteoblasts [21]. Moreover, MC3T3-E1 Subclone 4 forms a well mineralized ECM and exhibits high mRNAs expression for osteogenic markers, such as OC, parathyroid hormone (PTH)/parathyroid hormone-related protein (PTHrP) receptor and bone sialoprotein while cultured in presence of ascorbic acid and inorganic phosphate [22]. Whereas, the hFOB 1.19 cell line is considered a great cellular model, since it may differentiate into mature osteoblasts with the phenotype similar to normal primary osteoblasts [23].

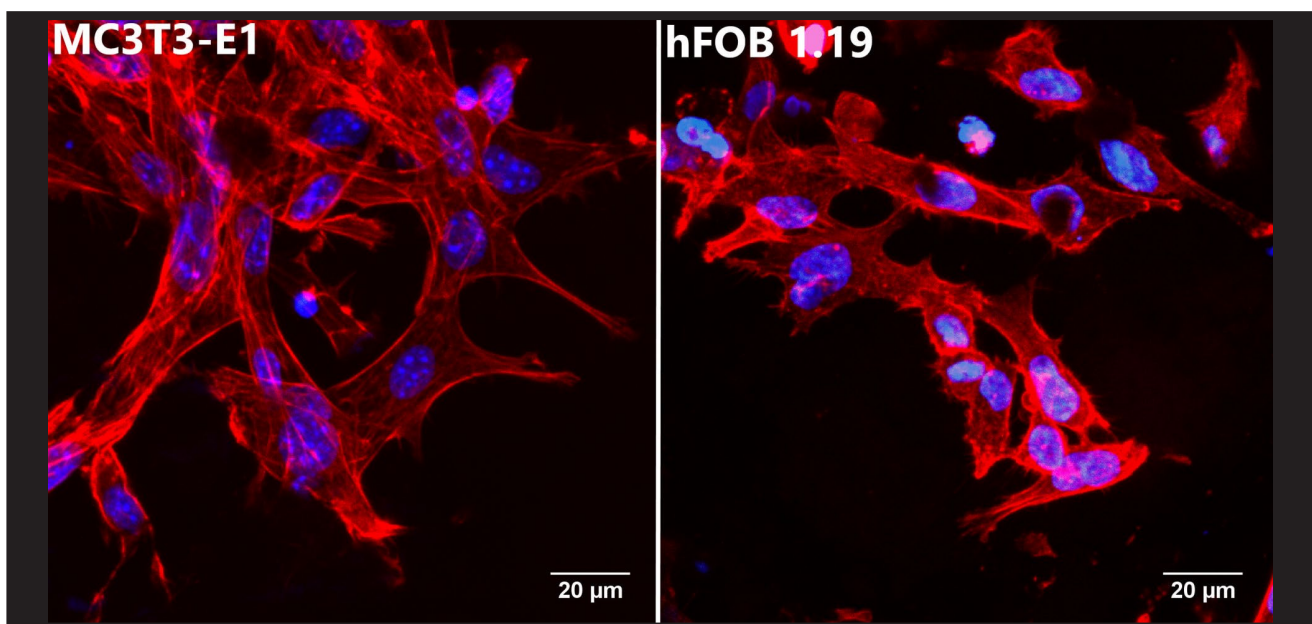


FIG. 4. Visualization of osteoblasts grown on the scaffold surface (cytoskeleton filaments – red fluorescence, nuclei – blue fluorescence; magn. 400x, scale bar = 20 μm).



In this research, the level of typical osteogenic markers (bALP, Col I, OC) produced by the MC3T3-E1 and the hFOB 1.19 cells cultured on the scaffold surface was estimated. The bALP activity was evaluated on the 8th and 16th day of the experiment since this enzyme is especially important for the second and the third stage of the differentiation process. Col I which is characteristic of the first and second stage was determined only on the 8th day, whereas OC, which is a late marker, was determined only on the 16th day of the experiment. The performed ELISAs clearly showed that the level of osteogenic markers which were synthesized by the cells cultured on the scaffold surface depended on the cell line type (FIG. 5).

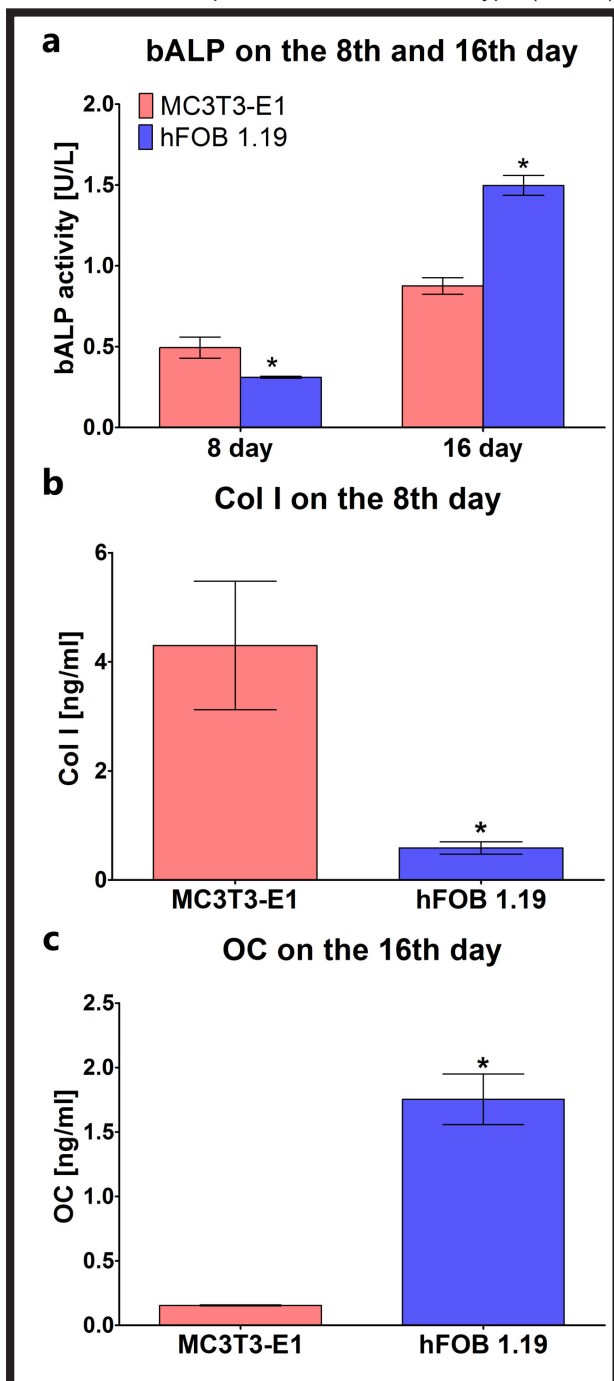


FIG. 5. Evaluation of osteogenic markers level: (a) bALP, (b) Col I, and (c) OC in MC3T3-E1 and hFOB 1.19 osteoblasts cultured on the surface of the scaffold for 8 and 16-days; \*statistically significant results compared to MC3T3-E1 cell line ( $p < 0.05$ ,  $n = 4$ , unpaired t-test).

It was observed that on the 16th day, the bALP activity increased when compared to the 8th day of the experiment for both cell lines (FIG. 5a). However, on the 16th day of the experiment, the hFOB 1.19 cells exhibited a significantly higher bALP activity than the MC3T3-E1 cells. Interestingly, the MC3T3-E1 cells produced a significantly higher amount of Col I than the hFOB 1.19 cells (FIG. 5b), whereas the hFOB 1.19 cells produced a significantly higher amount of OC than the MC3T3-E1 cells (FIG. 5c). Since human osteoblasts revealed the higher bALP activity (typical of 2 and 3 phase), they produced lower amounts of Col I (early differentiation marker, typical of 1 and 2 phase) and synthesized greater amounts of OC (late marker, typical of 3 phase) in comparison to mouse cells, it may be concluded that the hFOB 1.19 cells were in a more advanced phase of osteogenic differentiation than the MC3T3-E1 cells. The lower differentiation degree of the mouse cells cultured on the scaffold most likely resulted from the preosteoblast phenotype of MC3T3-E1 cells, as compared to human osteoblasts. According to the available literature, in contrast to the MC3T3-E1 cells, the differentiated hFOB 1.19 cells exhibit phenotype and gene expression typical of primary mature osteoblasts [6]. Importantly, the obtained results clearly demonstrated that the surface of the fabricated scaffold facilitated the osteogenic differentiation, confirming that the developed biomaterial has osteoconductive properties.

## Conclusions

The obtained results demonstrated that the fabricated scaffold composed of the chitosan-agarose matrix reinforced with hydroxyapatite nanopowder is characterized by biocompatibility and osteoconductivity. The scaffold allows for the attachment and growth of both the mouse calvarial preosteoblasts (MC3T3-E1 Subclone 4) and the normal human foetal osteoblasts (hFOB 1.19). The innovative biomaterial also promotes the production of osteogenic markers by the mentioned cells. Interestingly, the developed scaffold reveals the different ion reactivity in the culture medium dedicated for mouse cells in comparison to the medium for human osteoblasts. It was also proved that the cell lines may differ in the cellular response to the investigated biomaterial. Therefore, to yield more reliable results it is recommended to perform biological characterization of the novel scaffold using at least two various cellular models. The presented results indicate that the novel bone scaffold has a great potential to be used in bone regeneration applications, however further experiments need to be performed to fully confirm its biomedical usefulness.

## Acknowledgments

The authors report no conflicts of interest in this work. The study was supported by National Science Centre (NCN) in Poland within OPUS 16 grant no. UMO-2018/31/B/ST8/00945 and by using the equipment purchased within agreement no. POPW.01.03.00-06-010/09-00 Operational Program Development of Eastern Poland 2007–2013, Priority Axis I, Modern Economy, Operations 1.3. Innovations Promotion.

## ORCID iDs

P. Kazimierzczak: <https://orcid.org/0000-0002-5893-7168>  
 V. Vivcharenko: <https://orcid.org/0000-0002-1526-686X>  
 W. Truskiewicz: <https://orcid.org/0000-0003-0459-2560>  
 M. Wójcik: <https://orcid.org/0000-0002-1918-6912>  
 A. Przekora: <https://orcid.org/0000-0002-6076-1309>

## References

- [1] O'Brien F.J.: Biomaterials & scaffolds for tissue engineering. *Materials Today* 14(3) (2011) 88-95.
- [2] Stevens M.M.: Biomaterials for bone tissue engineering. *Materials Today* 11(5) (2008) 18-25.
- [3] Roseti L., Parisi V., Petretta M., Cavallo C., Desando G., Bartolotti I., Grigolo B.: Scaffolds for bone tissue engineering: State of the art and new perspectives. *Materials Science and Engineering C* 78 (2017) 1246-1262.
- [4] Thevenot P., Hu W., Tang L.: Surface chemistry influence implant. *Current Topics in Medical Chemistry* 8(4) (2008) 270-280.
- [5] Zivic F., Affatato S., Trajanovic M., Schnabelrauch M., Grujovic N., Choy K.L.: Biomaterials in clinical practice. *Advances in clinical research and medical devices*. Springer International Publishing AG, Switzerland 2018.
- [6] Przekora A.: The summary of the most important cell-biomaterial interactions that need to be considered during in vitro biocompatibility testing of bone scaffolds for tissue engineering applications. *Materials Science and Engineering C* 97 (2019) 1036-1051.
- [7] Karageorgiou V., Kaplan D.: Porosity of 3D biomaterial scaffolds and osteogenesis. *Biomaterials* 26 (27) (2005) 5474-5491.
- [8] Sachot N., Engel E., Castano O.: Hybrid organic-inorganic scaffolding biomaterials for regenerative therapies. *Current Organic Chemistry* 18 (18) (2014) 2299-2314.
- [9] Subia B., Kundu J., Kundu S.C.: Biomaterial scaffold fabrication techniques for potential tissue engineering applications. *Tissue Engineering, InTech Croatia* (2010) 141-158.
- [10] Chang H-I., Wang Y.: Cell responses to surface and architecture of tissue engineering scaffolds. *Regenerative Medicine and Tissue Engineering - Cells and Biomaterials*. InTech Croatia (2011) 569-588.
- [11] Rabe M., Verdes D., Seeger S.: Understanding protein adsorption phenomena at solid surfaces. *Advances in Colloid and Interface Science* 162(1-2) (2011) 87-106.
- [12] Kazimierczak P., Benko A., Palka K., Canal C., Kolodynska D., Przekora A.: Novel synthesis method combining a foaming agent with freeze-drying to obtain hybrid highly macroporous bone scaffolds. *Journal of Materials Science and Technology* (2020) article in press.
- [13] Przekora A., Ginalska G.: Enhanced differentiation of osteoblastic cells on novel chitosan/ $\beta$ -1,3-glucon/bioceramic scaffolds for bone tissue regeneration. *Biomedical Materials* 10(1) (2015).
- [14] Gustavsson J., Ginebra M.P., Engel E., Planell J.: Ion reactivity of calcium-deficient hydroxyapatite in standard cell culture media. *Acta Biomaterialia* 7(12) (2011) 4242-4252.
- [15] Przekora A., Czechowska J., Pijoch D., Ślósarczyk A., Ginalska G.: Do novel cement-type biomaterials reveal ion reactivity that affects cell viability in vitro? *Central European Journal of Biology* 9(3) (2014) 277-289.
- [16] Xu J., Liu L., Munroe P., Xie Z.H.: Promoting bone-like apatite formation on titanium alloys through nanocrystalline tantalum nitride coatings. *Journal of Materials Chemistry B* 3(19) (2015) 4082-4094.
- [17] Kim H.M., Himeno T., Kawashita M., Kokubo T., Nakamura T.: The mechanism of biomineralization of bone-like apatite on synthetic hydroxyapatite: an in vitro assessment. *Journal of the Royal Society Interface* 1(1) (2004) 17-22.
- [18] Shibata H., Yokoi T., Goto T., Kim III Y., Kawashita M., Kikuta K., Ohtsuki Ch.: Behavior of hydroxyapatite crystals in a simulated body fluid: effects of crystal face. *Journal of the Ceramic Society of Japan* 121(9) (2013) 807-812.
- [19] Cao N., Chen X.B., Schreyer D.J.: Influence of calcium ions on cell survival and proliferation in the context of an alginate hydrogel. *ISRN Chemical Engineering* (2012) 1-9.
- [20] Tang Z., Li X., Tan Y., Fan H., Zhang X.: The material and biological characteristics of osteoinductive calcium phosphate ceramics. *Regenerative Biomaterials* 5(1) (2018) 43-59.
- [21] Czekanska E.M., Stoddart M.J., Ralphs J.R., Richards R.G., Hayes J.S.: A phenotypic comparison of osteoblast cell lines versus human primary osteoblasts for biomaterials testing. *Journal of Biomedical Materials Research - Part A* 102 (8) (2014) 2636-2643.
- [22] American Type Culture Collection: MC3T3E1 Subclone 4 (ATCC® CRL2593™), [https://www.lgcstandards-atcc.org/products/all/CRL-2593.aspx?geo\\_country=pl#generalinformation](https://www.lgcstandards-atcc.org/products/all/CRL-2593.aspx?geo_country=pl#generalinformation), Accessed date: 15 July 2019.
- [23] Subramaniam M., Jalal S.M., Rickard D.J., Rickard D.J., Harris S.A., Bolander M.E., Spelsberg T. C.: Further characterization of human fetal osteoblastic hFOB 1.19 and hFOB/ER $\alpha$  cells: Bone formation in vivo and karyotype analysis using multicolor fluorescent in situ hybridization. *Journal of Cellular Biochemistry* 87(1) (2002) 9-15.